
**Calculation of micropitting load capacity
of cylindrical spur and helical gears —**

**Part 1:
Introduction and basic principles**

*Calcul de la capacité de charge aux micropiqûres des engrenages
cylindriques à dentures droite et hélicoïdale —*

Partie 1: Introduction et principes fondamentaux



Reference number
ISO/TR 15144-1:2010(E)

© ISO 2010

PDF disclaimer

This PDF file may contain embedded typefaces. In accordance with Adobe's licensing policy, this file may be printed or viewed but shall not be edited unless the typefaces which are embedded are licensed to and installed on the computer performing the editing. In downloading this file, parties accept therein the responsibility of not infringing Adobe's licensing policy. The ISO Central Secretariat accepts no liability in this area.

Adobe is a trademark of Adobe Systems Incorporated.

Details of the software products used to create this PDF file can be found in the General Info relative to the file; the PDF-creation parameters were optimized for printing. Every care has been taken to ensure that the file is suitable for use by ISO member bodies. In the unlikely event that a problem relating to it is found, please inform the Central Secretariat at the address given below.



COPYRIGHT PROTECTED DOCUMENT

© ISO 2010

All rights reserved. Unless otherwise specified, no part of this publication may be reproduced or utilized in any form or by any means, electronic or mechanical, including photocopying and microfilm, without permission in writing from either ISO at the address below or ISO's member body in the country of the requester.

ISO copyright office
Case postale 56 • CH-1211 Geneva 20
Tel. + 41 22 749 01 11
Fax + 41 22 749 09 47
E-mail copyright@iso.org
Web www.iso.org

Published in Switzerland

Contents

Page

Foreword	v
Introduction.....	vi
1 Scope	1
2 Normative references	1
3 Terms, definitions, symbols and units	2
3.1 Terms and definitions	2
3.2 Symbols and units.....	2
4 Definition of micropitting.....	5
5 Basic formulae	5
5.1 General	5
5.2 Safety factor against micropitting S_{λ}	5
5.3 Local specific lubricant film thickness $\lambda_{GF,Y}$	6
5.4 Permissible specific lubricant film thickness λ_{GFP}	7
5.5 Recommendation for the minimum safety factor against micropitting $S_{\lambda,min}$	7
6 Material parameter G_M	8
6.1 Reduced modulus of elasticity E_r	8
6.2 Pressure-viscosity coefficient at bulk temperature $\alpha_{\theta M}$	9
7 Velocity parameter U_Y	9
7.1 Sum of tangential velocities $v_{\Sigma,Y}$	10
7.2 Dynamic viscosity at bulk temperature $\eta_{\theta M}$	10
8 Load parameter W_Y	11
8.1 Local Hertzian contact stress $p_{dyn,Y,A}$ according to Method A	12
8.2 Local Hertzian contact stress $p_{dyn,Y,B}$ according to Method B	12
9 Sliding parameter $S_{GF,Y}$	13
9.1 Pressure-viscosity coefficient at local contact temperature $\alpha_{\theta B,Y}$	13
9.2 Dynamic viscosity at local contact temperature $\eta_{\theta B,Y}$	14
10 Definition of contact point Y on the path of contact.....	14
11 Load sharing factor X_Y	18
11.1 Spur gears with unmodified profiles	18
11.2 Spur gears with profile modification	19
11.3 Buttressing factor $X_{but,Y}$	20
11.4 Helical gears with $\varepsilon_{\beta} < 1$ and unmodified profiles	21
11.5 Helical gears with $\varepsilon_{\beta} < 1$ and profile modification	22
11.6 Helical gears with $\varepsilon_{\beta} \geq 1$ and unmodified profiles	23
11.7 Helical gears with $\varepsilon_{\beta} \geq 1$ and profile modification	24
12 Contact temperature $\theta_{B,Y}$	25
13 Flash temperature $\theta_{fl,Y}$	25
14 Bulk temperature θ_M	26
14.1 Mean coefficient of friction μ_m	27
14.2 Load losses factor H_v	28
14.3 Tip relief factor X_{Ca}	29
14.4 Lubrication factor X_S	30

Annex A (informative) Calculation of the permissible specific lubricant film thickness λ_{GFP} for oils with a micropitting test result according to FVA-Information Sheet 54/7	31
Annex B (informative) Example calculation	33
Bibliography	56

© ISO 2010

Foreword

ISO (the International Organization for Standardization) is a worldwide federation of national standards bodies (ISO member bodies). The work of preparing International Standards is normally carried out through ISO technical committees. Each member body interested in a subject for which a technical committee has been established has the right to be represented on that committee. International organizations, governmental and non-governmental, in liaison with ISO, also take part in the work. ISO collaborates closely with the International Electrotechnical Commission (IEC) on all matters of electrotechnical standardization.

International Standards are drafted in accordance with the rules given in the ISO/IEC Directives, Part 2.

The main task of technical committees is to prepare International Standards. Draft International Standards adopted by the technical committees are circulated to the member bodies for voting. Publication as an International Standard requires approval by at least 75 % of the member bodies casting a vote.

In exceptional circumstances, when a technical committee has collected data of a different kind from that which is normally published as an International Standard ("state of the art", for example), it may decide by a simple majority vote of its participating members to publish a Technical Report. A Technical Report is entirely informative in nature and does not have to be reviewed until the data it provides are considered to be no longer valid or useful.

Attention is drawn to the possibility that some of the elements of this document may be the subject of patent rights. ISO shall not be held responsible for identifying any or all such patent rights.

ISO/TR 15144-1 was prepared by Technical Committee ISO/TC 60, *Gears*, Subcommittee SC 2, *Gear capacity calculation*.

ISO/TR 15144 consists of the following parts, under the general title *Calculation of micropitting load capacity of cylindrical spur and helical gears*:

— *Part 1: Introduction and basic principles*

Introduction

This part of ISO/TR 15144 provides principles for the calculation of the micropitting load capacity of cylindrical involute spur and helical gears with external teeth.

The basis for the calculation of the micropitting load capacity of a gear set is the model of the minimum operating specific lubricant film thickness in the contact zone. There are many influence parameters, such as surface topology, contact stress level, and lubricant chemistry. Whilst these parameters are known to affect the performance of micropitting for a gear set, it must be stated that the subject area remains a topic of research and, as such, the science has not yet developed to allow these specific parameters to be included directly in the calculation methods. Furthermore, the correct application of tip and root relief (involute modification) has been found to greatly influence micropitting; the suitable values should therefore be applied. Surface finish is another crucial parameter. At present R_a is used, but other aspects such as R_z or skewness have been observed to have significant effects which could be reflected in the finishing process applied.

Although the calculation of specific lubricant film thickness does not provide a direct method for assessing micropitting load capacity, it can serve as an evaluation criterion when applied as part of a suitable comparative procedure based on known gear performance.

Calculation of micropitting load capacity of cylindrical spur and helical gears —

Part 1: Introduction and basic principles

1 Scope

This part of ISO/TR 15144 describes a procedure for the calculation of the micropitting load capacity of cylindrical gears with external teeth. It has been developed on the basis of testing and observation of oil-lubricated gear transmissions with modules between 3 mm and 11 mm and pitch line velocities of 8 m/s to 60 m/s. However, the procedure is applicable to any gear pair where suitable reference data is available, providing the criteria specified below are satisfied.

The formulae specified are applicable for driving as well as for driven cylindrical gears with tooth profiles in accordance with the basic rack specified in ISO 53. They are also applicable for teeth conjugate to other basic racks where the virtual contact ratio is less than $\varepsilon_{\alpha n} = 2,5$. The results are in good agreement with other methods for normal working pressure angles up to 25° , reference helix angles up to 25° and in cases where pitch line velocity is higher than 2 m/s.

This part of ISO/TR 15144 is not applicable for the assessment of types of gear tooth surface damage other than micropitting.

2 Normative references

The following referenced documents are indispensable for the application of this document. For dated references, only the edition cited applies. For undated references, the latest edition of the referenced document (including any amendments) applies.

ISO 53:1998, *Cylindrical gears for general and heavy engineering — Standard basic rack tooth profile*

ISO 1122-1:1998, *Vocabulary of gear terms — Part 1: Definitions related to geometry*

ISO 1328-1:1995, *Cylindrical gears — ISO system of accuracy — Part 1: Definitions and allowable values of deviations relevant to corresponding flanks of gear teeth*

ISO 6336-1:2006, *Calculation of load capacity of spur and helical gears — Part 1: Basic principles, introduction and general influence factors*

ISO 6336-2:2006, *Calculation of load capacity of spur and helical gears — Part 2: Calculation of surface durability (pitting)*

ISO 21771:2007, *Gears — Cylindrical involute gears and gear pairs — Concepts and geometry*

ISO/TR 13989-1:2000, *Calculation of scuffing load capacity of cylindrical, bevel and hypoid gears — Part 1: Flash temperature method*

3 Terms, definitions, symbols and units

3.1 Terms and definitions

For the purposes of this document, the terms and definitions given in ISO 1122-1, ISO 6336-1 and ISO 6336-2 apply.

3.2 Symbols and units

The symbols used in this document are given in Table 1. The units of length metre, millimetre and micrometre are chosen in accordance with common practice. The conversions of the units are already included in the given equations.

Table 1 — Symbols and units

Symbol	Description	Unit
a	centre distance	mm
B_{M1}	thermal contact coefficient of pinion	$N/(m \cdot s^{0.5} \cdot K)$
B_{M2}	thermal contact coefficient of wheel	$N/(m \cdot s^{0.5} \cdot K)$
b	face width	mm
C_{a1}	tip relief of pinion	μm
C_{a2}	tip relief of wheel	μm
C_{eff}	effective tip relief	μm
c_{M1}	specific heat per unit mass of pinion	$J/(kg \cdot K)$
c_{M2}	specific heat per unit mass of wheel	$J/(kg \cdot K)$
c'	maximum tooth stiffness per unit face width (single stiffness) of a tooth pair	$N/(mm \cdot \mu m)$
$c_{\gamma\alpha}$	mean value of mesh stiffness per unit face width	$N/(mm \cdot \mu m)$
d_{a1}	tip diameter of pinion	mm
d_{a2}	tip diameter of wheel	mm
d_{b1}	base diameter of pinion	mm
d_{b2}	base diameter of wheel	mm
d_{w1}	pitch diameter of pinion	mm
d_{w2}	pitch diameter of wheel	mm
d_{Y1}	Y-circle diameter of pinion	mm
d_{Y2}	Y-circle diameter of wheel	mm
E_r	reduced modulus of elasticity	N/mm^2
E_1	modulus of elasticity of pinion	N/mm^2
E_2	modulus of elasticity of wheel	N/mm^2
F_{bt}	nominal transverse load in plane of action (base tangent plane)	N
F_t	(nominal) transverse tangential load at reference cylinder per mesh	N
G_M	material parameter	—
g_Y	parameter on the path of contact (distance of point Y from point A)	mm
g_α	length of path of contact	mm
H_v	load losses factor	—

Table 1 (continued)

Symbol	Description	Unit
h_Y	local lubricant film thickness	μm
K_A	application factor	–
$K_{H\alpha}$	transverse load factor	–
$K_{H\beta}$	face load factor	–
K_V	dynamic factor	–
n_1	rotation speed of pinion	min^{-1}
P	transmitted power	kW
p_{et}	transverse base pitch on the path of contact	mm
$p_{\text{dyn},Y}$	local Hertzian contact stress including the load factors K	N/mm^2
$p_{H,Y}$	local nominal Hertzian contact stress	N/mm^2
R_a	effective arithmetic mean roughness value	μm
R_{a1}	arithmetic mean roughness value of pinion	μm
R_{a2}	arithmetic mean roughness value of wheel	μm
$S_{GF,Y}$	local sliding parameter	–
S_λ	safety factor against micropitting	–
$S_{\lambda,\text{min}}$	minimum required safety factor against micropitting	–
T_1	nominal torque at the pinion	Nm
U_Y	local velocity parameter	–
u	gear ratio	–
$v_{g,Y}$	local sliding velocity	m/s
$v_{r1,Y}$	local tangential velocity on pinion	m/s
$v_{r2,Y}$	local tangential velocity on wheel	m/s
$v_{\Sigma,C}$	sum of tangential velocities at pitch point	m/s
$v_{\Sigma,Y}$	sum of tangential velocities at point Y	m/s
W_W	material factor	–
W_Y	local load parameter	–
$X_{\text{but},Y}$	local buttressing factor	–
X_{Ca}	tip relief factor	–
X_L	lubricant factor	–
X_R	roughness factor	–
X_S	lubrication factor	–
X_Y	local load sharing factor	–
Z_E	elasticity factor	$(\text{N/mm}^2)^{0.5}$
z_1	number of teeth of pinion	–
z_2	number of teeth of wheel	–
α_t	transverse pressure angle	$^\circ$
α_{wt}	pressure angle at the pitch cylinder	$^\circ$
$\alpha_{\theta B,Y}$	pressure-viscosity coefficient at local contact temperature	m^2/N
$\alpha_{\theta M}$	pressure-viscosity coefficient at bulk temperature	m^2/N
α_{38}	pressure-viscosity coefficient at 38 °C	m^2/N
β_b	base helix angle	$^\circ$

Table 1 (continued)

Symbol	Description	Unit
ε_{\max}	maximum addendum contact ratio	–
ε_{α}	transverse contact ratio	–
$\varepsilon_{\alpha n}$	virtual contact ratio, transverse contact ratio of a virtual spur gear	–
ε_{β}	overlap ratio	–
ε_{γ}	total contact ratio	–
ε_1	addendum contact ratio of the pinion	–
ε_2	addendum contact ratio of the wheel	–
$\eta_{\theta B,Y}$	dynamic viscosity at local contact temperature	N·s/m ²
$\eta_{\theta M}$	dynamic viscosity at bulk temperature	N·s/m ²
$\eta_{\theta oil}$	dynamic viscosity at oil inlet/sump temperature	N·s/m ²
η_{38}	dynamic viscosity at 38 °C	N·s/m ²
$\theta_{B,Y}$	local contact temperature	°C
$\theta_{fl,Y}$	local flash temperature	°C
θ_M	bulk temperature	°C
θ_{oil}	oil inlet/sump temperature	°C
$\lambda_{GF,min}$	minimum specific lubricant film thickness in the contact area	–
$\lambda_{GF,Y}$	local specific lubricant film thickness	–
λ_{GFP}	permissible specific lubricant film thickness	–
λ_{GFT}	limiting specific lubricant film thickness of the test gears	–
λ_{M1}	specific heat conductivity of pinion	W/(m·K)
λ_{M2}	specific heat conductivity of wheel	W/(m·K)
μ_m	mean coefficient of friction	–
$\nu_{\theta B,Y}$	kinematic viscosity at local contact temperature	mm ² /s
$\nu_{\theta M}$	kinematic viscosity at bulk temperature	mm ² /s
ν_1	Poisson's ratio of pinion	–
ν_2	Poisson's ratio of wheel	–
ν_{100}	kinematic viscosity at 100 °C	mm ² /s
ν_{40}	kinematic viscosity at 40 °C	mm ² /s
ρ_{M1}	density of pinion	kg/m ³
ρ_{M2}	density of wheel	kg/m ³
$\rho_{n,C}$	normal radius of relative curvature at pitch diameter	mm
$\rho_{n,Y}$	normal radius of relative curvature at point Y	mm
$\rho_{t,Y}$	transverse radius of relative curvature at point Y	mm
$\rho_{t1,Y}$	transverse radius of curvature of pinion at point Y	mm
$\rho_{t2,Y}$	transverse radius of curvature of wheel at point Y	mm
$\rho_{\theta B,Y}$	density of lubricant at local contact temperature	kg/m ³
$\rho_{\theta M}$	density of lubricant at bulk temperature	kg/m ³
ρ_{15}	density of lubricant at 15 °C	kg/m ³
Subscripts to symbols		
parameter for any contact point Y in the contact area for Method A and on the path of contact for Method B; (all parameters subscript Y have to be calculated with local values)		

4 Definition of micropitting

Micropitting is a phenomenon that occurs in Hertzian type of rolling and sliding contact that operates in elastohydrodynamic or boundary lubrication regimes. Micropitting is influenced by operating conditions such as load, speed, sliding, temperature, surface topography, specific lubricant film thickness and chemical composition of the lubricant. Micropitting is more commonly observed on materials with a high surface hardness.

Micropitting is the generation of numerous surface cracks. The cracks grow at a shallow angle to the surface forming micropits. The micropits are small relative to the size of the contact zone, typically of the order 10 - 20 μm deep. The micropits can coalesce to produce a continuous fractured surface which appears as a dull, matte surface during unmagnified visual inspection.

Micropitting is the preferred name for this phenomenon, but it has also been referred to as grey staining, grey flecking, frosting and peeling. Illustrations of micropitting can be found in ISO 10825 [8].

Micropitting may arrest. However, if micropitting continues to progress, it may result in reduced gear tooth accuracy, increased dynamic loads and noise. If it does not arrest and continues to propagate it can develop into macropitting and other modes of gear failure.

5 Basic formulae

5.1 General

The calculation of micropitting load capacity is based on the local specific lubricant film thickness $\lambda_{GF,Y}$ in the contact area and the permissible specific lubricant film thickness λ_{GFP} [11]. It is assumed that micropitting can occur, when the minimum specific lubricant film thickness $\lambda_{GF,min}$ is lower than a corresponding critical value λ_{GFP} . Both values $\lambda_{GF,min}$ and λ_{GFP} shall be calculated separately for pinion and wheel in the contact area. It has to be recognized that the determination of the minimum specific lubricant film thickness and the permissible specific lubricant film thickness have to be based on the operating parameters.

The micropitting load capacity can be determined by comparing the minimum specific lubricant film thickness with the corresponding limiting value derived from gears in service or from specific gear testing. This comparison will be expressed by the safety factor S_λ which shall be equal or higher than a minimum safety factor against micropitting $S_{\lambda,min}$.

Micropitting mainly occurs in areas of negative specific sliding. Negative specific sliding is to be found along the path of contact (see Figure 1) between point A and C on the driving gear and between point C and E on the driven gear. Considering the influences of lubricant, surface roughness, geometry of the gears and operating conditions the specific lubricant film thickness $\lambda_{GF,Y}$ can be calculated for every point in the field of contact.

5.2 Safety factor against micropitting S_λ

To account for the micropitting load capacity the safety factor S_λ according to equation (1) is defined.

$$S_\lambda = \frac{\lambda_{GF,min}}{\lambda_{GFP}} \geq S_{\lambda,min} \quad (1)$$

where

- $\lambda_{GF,min}$ = $\min(\lambda_{GF,Y})$ is the minimum specific lubricant film thickness in the contact area;
- $\lambda_{GF,Y}$ is the local specific lubricant film thickness (see 5.3);
- λ_{GFP} is the permissible specific lubricant film thickness (see 5.4);
- $S_{\lambda,min}$ is the minimum required safety factor (see 5.5).

The minimum specific lubricant film thickness is determined from all calculated local values of the specific lubricant film thickness $\lambda_{GF,Y}$ obtained by equation (2).

5.3 Local specific lubricant film thickness $\lambda_{GF,Y}$

For the determination of the safety factor S_λ the local lubricant film thickness h_Y according to Dowson/Higginson [5] in the field of contact has to be known and compared with the effective surface roughness.

$$\lambda_{GF,Y} = \frac{h_Y}{Ra} \quad (2)$$

where

$$Ra = 0,5 \cdot (Ra_1 + Ra_2) \quad (3)$$

$$h_Y = 1600 \cdot \rho_{n,Y} \cdot G_M^{0,6} \cdot U_Y^{0,7} \cdot W_Y^{-0,13} \cdot S_{GF,Y}^{0,22} \quad (4)$$

- Ra is the effective arithmetic mean roughness value;
- Ra_1 is the arithmetic mean roughness value of pinion (compare ISO 6336-2);
- Ra_2 is the arithmetic mean roughness value of wheel (compare ISO 6336-2);
- h_Y is the local lubricant film thickness;
- $\rho_{n,Y}$ is the normal radius of relative curvature at point Y (see clause 10);
- G_M is the material parameter (see clause 6);
- U_Y is the local velocity parameter (see clause 7);
- W_Y is the local load parameter (see clause 8);
- $S_{GF,Y}$ is the local sliding parameter (see clause 9).

Equation (4) should be calculated in the case of Method B at the seven local points (Y) defined in 5.3 b) using the values for $\rho_{n,Y}$, U_Y , W_Y and $S_{GF,Y}$ that exists at each point Y. The minimum of the seven h_Y ($\lambda_{GF,Y}$) values shall be used in equation (1).

An example calculation is presented in Annex B.

a) Method A

The local specific lubricant film thickness can be determined in the complete contact area by any appropriate gear computing program. In order to determine the local specific lubricant film thickness, the load distribution, the influence of normal and sliding velocity with changes of meshing phase and the actual service conditions shall be taken into consideration.

b) Method B

This method involves the assumption that the determinant local specific lubricant film thickness occurs on the tooth flank in the area of negative sliding. For simplification the calculation of the local specific lubricant film thickness is limited to certain points on the path of contact. For this purpose the lower point A and upper point E on the path of contact, the lower point B and upper point D of single pair tooth contact, the midway point AB between A and B, the midway point DE between D and E as well as the pitch point C are surveyed.

5.4 Permissible specific lubricant film thickness λ_{GFP}

For the determination of the permissible specific lubricant film thickness λ_{GFP} different procedures are applicable.

a) Method A

For Method A experimental investigations or service experience relating to micropitting on real gears are used.

Running real gears under conditions where micropitting just occurs the minimum specific lubricant film thickness can be calculated according to 5.3 a). This value is equivalent to the limiting specific lubricant film thickness which is used to calculate the micropitting load capacity.

Such experimental investigations may be performed on gears having the same design as the actual gear pair. In this case the gear manufacturing, gear accuracy, operating conditions, lubricant and operating temperature have to be appropriate for the actual gear box.

The cost required for this method is in general only justifiable for the development of new products as well as for gear boxes where failure would have serious consequences.

Otherwise the permissible specific lubricant film thickness λ_{GFP} may be derived from consideration of dimensions, service conditions and performance of carefully monitored reference gears operated with the respective lubricant. The more closely the dimensions and service conditions of the actual gears resemble those of the reference gears, the more effective will be the application of such values for the purpose of design ratings or calculation checks.

b) Method B

The method adapted is validated by carrying out careful comparative studies of well-documented histories of a number of test gears applicable to the type, quality and manufacture of gearing under consideration. The permissible specific lubricant film thickness λ_{GFP} is calculated from the critical specific lubricant film thickness λ_{GFT} which is the result of any standardised test method applicable to evaluate the micropitting load capacity of lubricants or materials by means of defined test gears operated under specified test conditions. λ_{GFT} is a function of the temperature, oil viscosity, base oil and additive chemistry and can be calculated according to equation (2) in the contact point of the defined test gears where the minimum specific lubricant film thickness is to be found and for the test conditions where the failure limit concerning micropitting in the standardised test procedure has been reached.

The test gears as well as the test conditions (for example the test temperature) have to be appropriate for the real gears in consideration.

Any standardised test can be used to determine the data. Where a specific test procedure is not available or required, a number of internationally available standardised test methods for the evaluation of micropitting performance of gears, lubricants and materials are currently available. Some widely used test procedures are the FVA-FZG-micropitting test [7], Flender micropitting test [12], BGA-DU micropitting test [2] and the micropitting test according to [3]. Annex A provides some generalised test data (for reference only) that have been produced using the test procedure according to FVA-Information Sheet 54/7 [7] where a value for λ_{GFP} can be calculated for a generalised reference allowable using equation A.1.

5.5 Recommendation for the minimum safety factor against micropitting $S_{\lambda,\text{min}}$

For a given application, adequate micropitting load capacity is demonstrated by the computed value of S_{λ} and being greater than or equal to the value $S_{\lambda,\text{min}}$, respectively.

Certain minimum values for the safety factor shall be determined. Recommendations concerning these minimum values are made in the following, but values are not proposed.

An appropriate probability of failure and the safety factor shall be carefully chosen to meet the required reliability at a justifiable cost. If the performance of the gears can be accurately appraised through testing of the actual unit under actual load conditions, a lower safety factor and more economical manufacturing procedures may be permissible:

$$\text{Safety factor} = \frac{\text{Calculated minimum specific film thickness}}{\text{Permissible specific film thickness}}$$

In addition to the general requirements mentioned and the special requirements for specific lubricant film thickness, the safety factor shall be chosen after careful consideration of the following influences.

- reliability of load values used for calculation: If loads or the response of the system to vibration, are estimated rather than measured, a larger safety factor should be used.
- variations in gear geometry and surface texture due to manufacturing tolerances,
- variations in alignment,
- variations in material due to process variations in chemistry, cleanliness and microstructure (material quality and heat treatment),
- variations in lubrication and its maintenance over the service life of the gears.

Depending on the reliability of the assumptions on which the calculations are based (for example load assumptions) and according to the reliability requirements (consequences of occurrence), a corresponding safety factor is to be chosen.

Where gears are produced according to a specification or a request for proposal (quotation), in which the gear supplier is to provide gears or assembled gear drives having specified calculated capacities (ratings) in accordance with this technical report, the value of the safety factor for micropitting is to be agreed upon between the parties.

6 Material parameter G_M

The material parameter G_M accounts for the influence of the reduced modulus of elasticity E_r and the pressure-viscosity coefficient of the lubricant at bulk temperature $\alpha_{\theta M}$.

$$G_M = 10^6 \cdot \alpha_{\theta M} \cdot E_r \tag{5}$$

where

E_r is the reduced modulus of elasticity (see 6.1);

$\alpha_{\theta M}$ is the pressure-viscosity coefficient at bulk temperature (see 6.2).

6.1 Reduced modulus of elasticity E_r

For mating gears of different material and modulus of elasticity E_1 and E_2 , the reduced modulus of elasticity E_r can be determined by equation (6). For mating gears of the same material $E = E_1 = E_2$ equation (7) may be used.

$$E_r = 2 \cdot \left(\frac{1 - \nu_1^2}{E_1} + \frac{1 - \nu_2^2}{E_2} \right)^{-1} \tag{6}$$

$$E_r = \frac{E}{1-\nu^2} \quad \text{for } E_1 = E_2 = E \text{ and } \nu_1 = \nu_2 = \nu \quad (7)$$

where

E_1 is the modulus of elasticity of pinion (for steel: $E = 206000 \text{ N/mm}^2$);

E_2 is the modulus of elasticity of wheel (for steel: $E = 206000 \text{ N/mm}^2$);

ν_1 is the Poisson's ratio of pinion (for steel: $\nu = 0,3$);

ν_2 is the Poisson's ratio of wheel (for steel: $\nu = 0,3$).

6.2 Pressure-viscosity coefficient at bulk temperature $\alpha_{\theta M}$

If the data for the pressure-viscosity coefficient at bulk temperature $\alpha_{\theta M}$ for the specific lubricant is not available, it can be approximated by equation (8) (see [9]).

$$\alpha_{\theta M} = \alpha_{38} \cdot \left[1 + 516 \cdot \left(\frac{1}{\theta_M + 273} - \frac{1}{311} \right) \right] \quad (8)$$

where

α_{38} is the pressure-viscosity coefficient of the lubricant at $38 \text{ }^\circ\text{C}$;

θ_M is the bulk temperature (see clause 14).

If no values for α_{38} are available then the following approximated values [1] can be used.

$$\alpha_{38} = 2,657 \cdot 10^{-8} \cdot \eta_{38}^{0,1348} \quad \text{for mineral oil} \quad (9)$$

$$\alpha_{38} = 1,466 \cdot 10^{-8} \cdot \eta_{38}^{0,0507} \quad \text{for PAO - based synthetic non-VI improved oil} \quad (10)$$

$$\alpha_{38} = 1,392 \cdot 10^{-8} \cdot \eta_{38}^{0,1572} \quad \text{for PAG - based synthetic oil} \quad (11)$$

where

η_{38} is the dynamic viscosity of the lubricant at $38 \text{ }^\circ\text{C}$.

7 Velocity parameter U_Y

The velocity parameter U_Y describes the proportional increase of the specific lubricant film thickness with increasing dynamic viscosity $\eta_{\theta M}$ of the lubricant at bulk temperature and sum of the tangential velocities $v_{\Sigma, Y}$.

$$U_Y = \eta_{\theta M} \cdot \frac{v_{\Sigma, Y}}{2000 \cdot E_r \cdot \rho_{n, Y}} \quad (12)$$

where

$\eta_{\theta M}$ is the dynamic viscosity of the lubricant at bulk temperature (see 7.2);

$v_{\Sigma, Y}$ is the sum of the tangential velocities (see 7.1);

E_r is the reduced modulus of elasticity (see 6.1);

$\rho_{n, Y}$ is the local normal radius of relative curvature (see clause 10).

7.1 Sum of tangential velocities $v_{\Sigma,Y}$

The sum of the tangential velocities at a mesh point Y is calculated according to equation (13). The velocity for pinion $v_{r1,Y}$ and wheel $v_{r2,Y}$ in a certain contact point Y on the tooth flank depends on the diameter at pinion d_{Y1} and the diameter at wheel d_{Y2} of point Y.

$$v_{\Sigma,Y} = v_{r1,Y} + v_{r2,Y} \quad (13)$$

where

$$v_{r1,Y} = 2 \cdot \pi \cdot \frac{n_1}{60} \cdot \frac{d_{w1}}{2000} \cdot \sin \alpha_{wt} \cdot \sqrt{\frac{d_{Y1}^2 - d_{b1}^2}{d_{w1}^2 - d_{b1}^2}} \quad (14)$$

$$v_{r2,Y} = 2 \cdot \pi \cdot \frac{n_1}{u \cdot 60} \cdot \frac{d_{w2}}{2000} \cdot \sin \alpha_{wt} \cdot \sqrt{\frac{d_{Y2}^2 - d_{b2}^2}{d_{w2}^2 - d_{b2}^2}} \quad (15)$$

- $v_{r1,Y}$ is the tangential velocity on pinion (see Figure 1);
- $v_{r2,Y}$ is the tangential velocity on wheel (see Figure 1);
- d_{b1} is the base diameter of pinion;
- d_{b2} is the base diameter of wheel;
- d_{w1} is the pitch diameter of pinion;
- d_{w2} is the pitch diameter of wheel;
- d_{Y1} is the Y-circle diameter of pinion (see Figure 1 and clause 10);
- d_{Y2} is the Y-circle diameter of wheel (see Figure 1 and clause 10);
- n_1 is the rotation speed of pinion;
- $u = z_2/z_1$ is the gear ratio;
- α_{wt} is the pressure angle at the pitch cylinder.

7.2 Dynamic viscosity at bulk temperature $\eta_{\theta M}$

The dynamic viscosity at bulk temperature $\eta_{\theta M}$ can be calculated according to equation (16).

$$\eta_{\theta M} = 10^{-6} \cdot \nu_{\theta M} \cdot \rho_{\theta M} \quad (16)$$

where

- $\nu_{\theta M}$ is the kinematic viscosity of the lubricant at bulk temperature (see 7.2.1);
- $\rho_{\theta M}$ is the density of the lubricant at bulk temperature (see 7.2.2).

7.2.1 Kinematic viscosity at bulk temperature $\nu_{\theta M}$

The kinematic viscosity at bulk temperature $\nu_{\theta M}$ can be calculated from the kinematic viscosity ν_{40} at 40 °C and the kinematic viscosity ν_{100} at 100 °C on the basis of equation (17). Extrapolation for temperature higher than 140 °C should be confirmed by measurement.

$$\log[\log(\nu_{\theta_M} + 0,7)] = A \cdot \log(\theta_M + 273) + B \quad (17)$$

where

$$A = \frac{\log[\log(\nu_{40} + 0,7)/\log(\nu_{100} + 0,7)]}{\log(313/373)} \quad (18)$$

$$B = \log[\log(\nu_{40} + 0,7)] - A \cdot \log(313) \quad (19)$$

θ_M is the bulk temperature (see clause 14);

ν_{40} is the kinematic viscosity of the lubricant at 40 °C;

ν_{100} is the kinematic viscosity of the lubricant at 100 °C.

7.2.2 Density of the lubricant at bulk temperature ρ_{θ_M}

If the density of the lubricant at bulk temperature ρ_{θ_M} is not available, it can be approximated based on the density of the lubricant at 15 °C according to equation (20).

$$\rho_{\theta_M} = \rho_{15} \cdot \left[1 - 0,7 \cdot \frac{(\theta_M + 273) - 289}{\rho_{15}} \right] \quad (20)$$

where

ρ_{15} is the density of the lubricant at 15 °C according to the lubricant data sheet;

θ_M is the bulk temperature (see clause 14).

If no data for ρ_{15} is available then equation (21) may be used for approximation of mineral oils.

$$\rho_{15} = 43,37 \cdot \log \nu_{40} + 805,5 \quad (21)$$

ν_{40} is the kinematic viscosity of the lubricant at 40 °C.

8 Load parameter W_Y

The load parameter W_Y can be determined using the local Hertzian contact stress $p_{\text{dyn},Y}$ and the reduced modulus of elasticity E_r .

$$W_Y = \frac{2 \cdot \pi \cdot p_{\text{dyn},Y}^2}{E_r^2} \quad (22)$$

where

$\pi_{\text{dyn},Y}$ is the local Hertzian contact stress according to Method A (see 8.1) or according to Method B (see 8.2);

E_r is the reduced modulus of elasticity (see 6.1).

8.1 Local Hertzian contact stress $p_{\text{dyn},Y,A}$ according to Method A

The local Hertzian contact stress $p_{\text{dyn},Y,A}$ according to Method A should be determined by means of a 3D mesh contact and load distribution analysis procedure. The local nominal Hertzian contact stress determined from the elastic mesh contact model $p_{H,Y,A}$ is applied to equation (23) to obtain the local Hertzian contact stress $p_{\text{dyn},Y,A}$.

$$p_{\text{dyn},Y,A} = p_{H,Y,A} \cdot \sqrt{K_A \cdot K_v} \quad (23)$$

where

$p_{H,Y,A}$ is the local nominal Hertzian contact stress, calculated with a 3D load distribution program;

K_A is the application factor (according to ISO 6336-1);

K_v is the dynamic factor (according to ISO 6336-1).

NOTE Where either K_A or K_v influences are already considered in the 3D elastic mesh contact model either or both K_A and K_v should be set as 1,0 in equation (23).

8.2 Local Hertzian contact stress $p_{\text{dyn},Y,B}$ according to Method B

The local Hertzian contact stress $p_{\text{dyn},Y,B}$ according to Method B is calculated according to equation (24). The required nominal Hertzian contact stress $p_{H,Y,B}$ is obtained by equation (25), see 8.2.1. The total load in the case of drive trains with multiple transmission paths or planetary gear systems is not quite evenly distributed over the individual meshes. This is to be taken into consideration by inserting a distribution factor K_γ to follow K_A in equation (24), to adjust the average load per mesh as necessary.

$$p_{\text{dyn},Y,B} = p_{H,Y,B} \cdot \sqrt{K_A \cdot K_v \cdot K_{H\alpha} \cdot K_{H\beta}} \quad (24)$$

where

$p_{H,Y,B}$ is the local nominal Hertzian contact stress (see 8.2.1);

K_A is the application factor (according to ISO 6336-1);

K_v is the dynamic factor (according to ISO 6336-1);

$K_{H\alpha}$ is the transverse load factor (according to ISO 6336-1). Profile modifications are considered in the factor X_γ , see clause 11.

$K_{H\beta}$ is the face load factor (according to ISO 6336-1). Lead modifications are considered in this factor.

NOTE Gears with a total contact ratio $\varepsilon_\gamma > 2$ can only be calculated according to Method A.

8.2.1 Nominal Hertzian contact stress $p_{H,Y,B}$

The nominal Hertzian contact stress $p_{H,Y,B}$ is used to determine the local Hertzian contact stress $p_{\text{dyn},Y,B}$ (see 8.1). To take the influence of different profile modifications into account the load sharing factor X_γ is introduced. For the calculation of the local nominal Hertzian contact stress the local nominal radius of relative curvature is used.

$$p_{H,Y,B} = Z_E \cdot \sqrt{\frac{F_t \cdot X_\gamma}{b \cdot \rho_{n,Y} \cdot \cos \alpha_t \cdot \cos \beta_b}} \quad (25)$$

where

$$Z_E = \sqrt{\frac{E_r}{2\pi}} \quad (26)$$

- Z_E is the elasticity factor (according to ISO 6336-2);
- b is the face width;
- F_t is the transverse tangential load at reference cylinder;
- X_Y is the load sharing factor (see clause 11);
- E_r is the reduced modulus of elasticity (see 6.1);
- α_t is the transverse pressure angle;
- β_b is the base helix angle;
- $\rho_{h,Y}$ is the local normal radius of relative curvature (see clause 10).

9 Sliding parameter $S_{GF,Y}$

The sliding parameter $S_{GF,Y}$ accounts for the influence of local sliding on the local temperature. This temperature influences both the local pressure-viscosity coefficient and the local dynamic viscosity and hence the local lubricant film thickness [6]. The indices “ $\theta_{B,Y}$ ” for local contact temperature and “ θ_M ” for bulk temperature are used. The local contact temperature $\theta_{B,Y}$ is the sum of the local flash $\theta_{h,Y}$ and the bulk temperature θ_M .

$$S_{GF,Y} = \frac{\alpha_{\theta_{B,Y}} \cdot \eta_{\theta_{B,Y}}}{\alpha_{\theta_M} \cdot \eta_{\theta_M}} \quad (27)$$

where

- $\alpha_{\theta_{B,Y}}$ is the pressure-viscosity coefficient at local contact temperature (see 9.1);
- $\eta_{\theta_{B,Y}}$ is the dynamic viscosity at local contact temperature (see 9.2);
- α_{θ_M} is the pressure-viscosity coefficient at bulk temperature (see 6.2);
- η_{θ_M} is the dynamic viscosity at bulk temperature (see 7.2).

9.1 Pressure-viscosity coefficient at local contact temperature $\alpha_{\theta_{B,Y}}$

If the data for the pressure-viscosity coefficient at local contact temperature $\alpha_{\theta_{B,Y}}$ for the specific lubricant is not available, it can be approximated by equation (28) (see [9]).

$$\alpha_{\theta_{B,Y}} = \alpha_{38} \cdot \left[1 + 516 \cdot \left(\frac{1}{\theta_{B,Y} + 273} - \frac{1}{311} \right) \right] \quad (28)$$

where

- α_{38} is the pressure-viscosity coefficient of the lubricant at 38 °C (see also 6.2);
- $\theta_{B,Y}$ is the local contact temperature (see clause 12).

9.2 Dynamic viscosity at local contact temperature $\eta_{\theta_{B,Y}}$

The dynamic viscosity at local contact temperature $\eta_{\theta_{B,Y}}$ is determined by equation (29).

$$\eta_{\theta_{B,Y}} = 10^{-6} \cdot \nu_{\theta_{B,Y}} \cdot \rho_{\theta_{B,Y}} \quad (29)$$

where

$\nu_{\theta_{B,Y}}$ is the kinematic viscosity at local contact temperature (see 9.2.1);

$\rho_{\theta_{B,Y}}$ is the density of the lubricant at local contact temperature (see 9.2.2).

9.2.1 Kinematic viscosity at local contact temperature $\nu_{\theta_{B,Y}}$

The kinematic viscosity at local contact temperature $\nu_{\theta_{B,Y}}$ can be calculated from the kinematic viscosity ν_{40} at 40 °C and the kinematic viscosity ν_{100} at 100 °C on the basis of equation (30). Extrapolation for temperature higher than 140 °C should be confirmed by measurement.

$$\log[\log(\nu_{\theta_{B,Y}} + 0,7)] = A \cdot \log(\theta_{B,Y} + 273) + B \quad (30)$$

where

$$A = \frac{\log[\log(\nu_{40} + 0,7) / \log(\nu_{100} + 0,7)]}{\log(313 / 373)} \quad (31)$$

$$B = \log[\log(\nu_{40} + 0,7)] - A \cdot \log(313) \quad (32)$$

$\theta_{B,Y}$ is the local contact temperature (see clause 12);

ν_{40} is the kinematic viscosity of the lubricant at 40 °C;

ν_{100} is the kinematic viscosity of the lubricant at 100 °C.

9.2.2 Density of the lubricant at local contact temperature $\rho_{\theta_{B,Y}}$

If the density of the lubricant at local contact temperature $\rho_{\theta_{B,Y}}$ is not available, it can be approximated based on the density of the lubricant at 15 °C according to equation (33).

$$\rho_{\theta_{B,Y}} = \rho_{15} \cdot \left[1 - 0,7 \cdot \frac{(\theta_{B,Y} + 273) - 289}{\rho_{15}} \right] \quad (33)$$

where

ρ_{15} is the density of the lubricant at 15 °C according to the lubricant data sheet (see also 7.2.2);

$\theta_{B,Y}$ is the local contact temperature (see clause 12).

10 Definition of contact point Y on the path of contact

Contact point Y is located between the SAP (contact point A) and EAP (contact point E) on the path of contact according to Figure 1. It describes the actual contact point between pinion and wheel in a certain meshing position g_Y .

According to 5.3, Method B the calculation has to be done for the following contact points:

Y =

- **A** $g_Y = g_A = 0$ mm the lower point on the path of contact (34)
- **AB** $g_Y = g_{AB} = (g_\alpha - \rho_{et}) / 2$ the midway point between A and B (35)
- **B** $g_Y = g_B = g_\alpha - \rho_{et}$ the lower point of single pair tooth contact (36)
- **C** $g_Y = g_C = \frac{d_{b1}}{2} \cdot \tan \alpha_{wt} - \sqrt{\frac{d_{a1}^2}{4} - \frac{d_{b1}^2}{4}} + g_\alpha$ the pitch point (37)
- **D** $g_Y = g_D = \rho_{et}$ the upper point of single pair tooth contact (38)
- **DE** $g_Y = g_{DE} = (g_\alpha - \rho_{et}) / 2 + \rho_{et}$ the midway point between D and E (39)
- **E** $g_Y = g_E = g_\alpha$ the upper point on the path of contact (40)

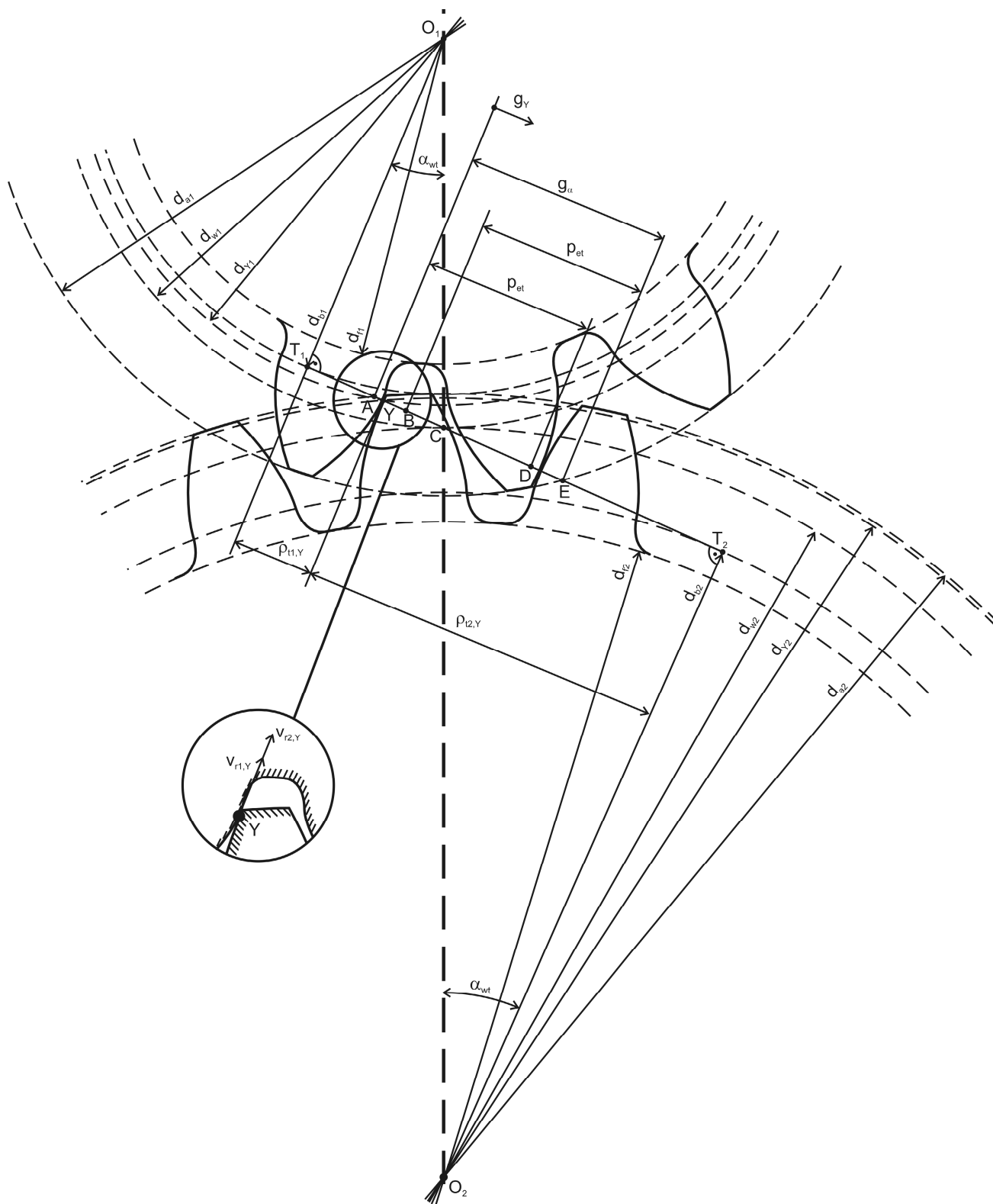


Figure 1 — Definition of contact point Y on the line of action

The Y-circle diameter of pinion d_{Y1} and wheel d_{Y2} are dependent on the location of contact point Y on the path of contact g_Y and can be calculated according to equation (41) and equation (42).

$$d_{Y1} = 2 \cdot \sqrt{\frac{d_{b1}^2}{4} + \left(\sqrt{\frac{d_{a1}^2}{4} - \frac{d_{b1}^2}{4}} - g_\alpha + g_Y \right)^2} \quad (41)$$

$$d_{Y2} = 2 \cdot \sqrt{\frac{d_{b2}^2}{4} + \left(\sqrt{\frac{d_{a2}^2}{4} - \frac{d_{b2}^2}{4}} - g_Y \right)^2} \quad (42)$$

where

d_{a1} is the tip diameter of pinion (see Figure 1);

d_{a2} is the tip diameter of wheel (see Figure 1);

d_{b1} is the base diameter of pinion (see Figure 1);

d_{b2} is the base diameter of wheel (see Figure 1);

g_Y is the parameter on the path of contact (see Figure 1);

g_α is the length of path of contact (see Figure 1).

The transverse radius of relative curvature $\rho_{t,Y}$ can be determined according to equation (43).

$$\rho_{t,Y} = \frac{\rho_{t1,Y} \cdot \rho_{t2,Y}}{\rho_{t1,Y} + \rho_{t2,Y}} \quad (43)$$

where

$$\rho_{t1,2,Y} = \sqrt{\frac{d_{Y1,2}^2 - d_{b1,2}^2}{4}} \quad (44)$$

$\rho_{t1,2,Y}$ is the transverse radius of curvature of pinion/ wheel at point Y (see Figure 1);

$d_{b1,2}$ is the base diameter of pinion/ wheel (see Figure 1);

$d_{Y1,2}$ is the Y-circle diameter of pinion/ wheel (see above and Figure 1).

The normal radius of relative curvature $\rho_{n,Y}$ can be calculated according to equation (45).

$$\rho_{n,Y} = \frac{\rho_{t,Y}}{\cos \beta_b} \quad (45)$$

where

$\rho_{t,Y}$ is the transverse relative radius of curvature (see above);

β_b is the base helix angle.

11 Load sharing factor X_Y

The load sharing factor X_Y accounts for the load sharing of succeeding pairs of meshing teeth. The load sharing factor is presented as a function of the linear parameter g_Y on the path of contact [4].

Due to inaccuracies a preceding pair of meshing teeth may cause an instantaneous increase or decrease of the theoretical load sharing factor, independent of the instantaneous increase or decrease caused by inaccuracies of a succeeding pair of meshing teeth at a later time. The value of X_Y does not exceed 1,0 (for cylindrical gears), which means full transverse single tooth contact. The region of transverse single tooth contact may be extended by an irregularly varying location of a dynamic load.

The load sharing factor X_Y depends on the type of gear transmission and on the profile modification. In case of buttressing of helical teeth (no profile modification) the load sharing factor is combined with a buttressing factor $X_{but,Y}$ [4].

11.1 Spur gears with unmodified profiles

The load sharing factor for a spur gear with unmodified profile is conventionally supposed to have a discontinuous trapezoidal shape; see Figure 2. However, due to manufacturing inaccuracies, in each path of double contact the load sharing factor will increase for protruding flanks and decrease for other flanks. The representative load sharing factor is an envelope of possible curves; see Figure 3.

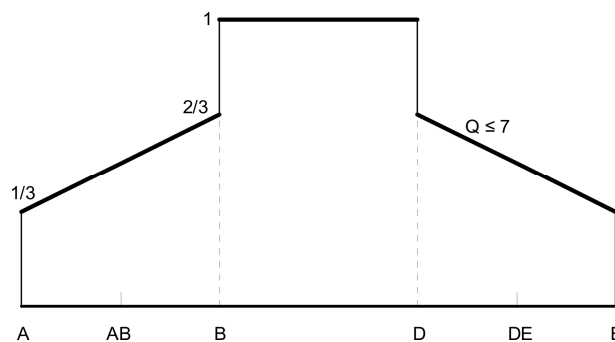


Figure 2 — Load sharing factor for cylindrical spur gears with unmodified profiles and quality grade ≤ 7

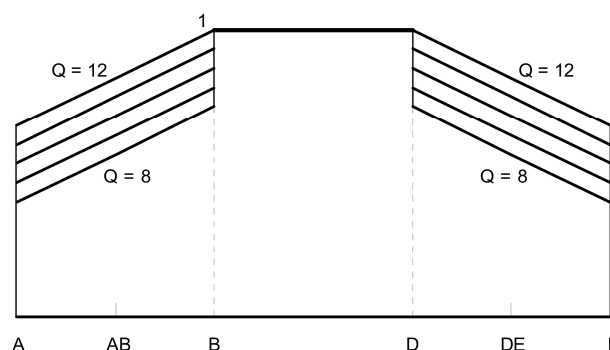


Figure 3 — Load sharing factor for cylindrical spur gears with unmodified profiles and quality grade ≥ 8

$$X_Y = \frac{Q-2}{15} + \frac{1}{3} \cdot \frac{g_Y}{g_B} \quad \text{for } g_A \leq g_Y < g_B \quad (46)$$

$$X_Y = 1,0 \quad \text{for } g_B \leq g_Y \leq g_D \quad (47)$$

$$X_Y = \frac{Q-2}{15} + \frac{1}{3} \cdot \frac{g_a - g_Y}{g_a - g_D} \quad \text{for } g_D < g_Y \leq g_E \quad (48)$$

where

Q = 7 for quality grade ≤ 7;

Q = equals quality grade for grade ≥ 8.

11.2 Spur gears with profile modification

See Figure 4, Figure 5 and Figure 6.

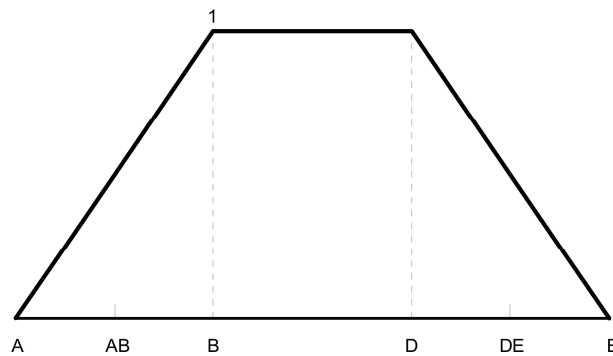


Figure 4 — Load sharing factor for cylindrical spur gears with optimum profile modification

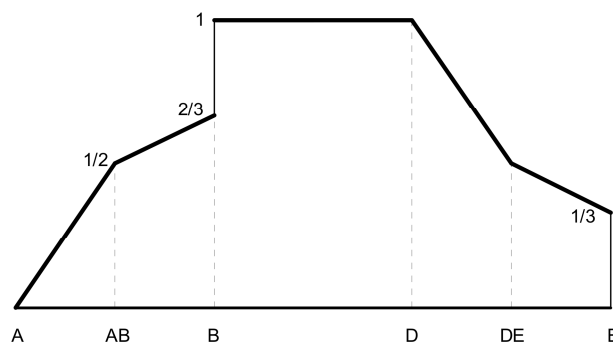


Figure 5 — Load sharing factor for cylindrical spur gears with optimum profile modification on the addendum of the driven gear and/or the dedendum of the driving gear

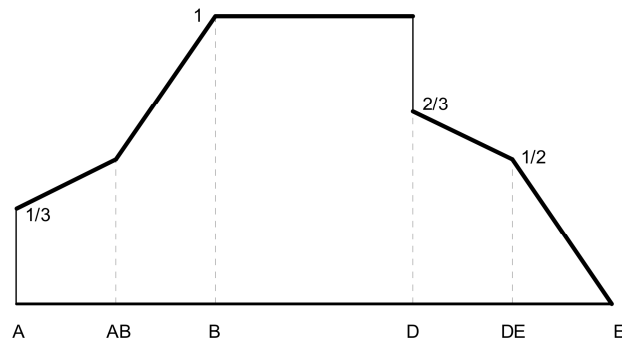


Figure 6 — Load sharing factor for cylindrical spur gears with optimum profile modification on the addendum of the driving gear and/or the dedendum of the driven gear

Linear interpolation between the values is possible.

$$X_Y = \frac{1}{3} + \frac{1}{3} \cdot \frac{g_Y}{g_B} \quad \text{for } g_A \leq g_Y \leq g_{AB} \quad \text{if } C_{a2} = 0 \mu\text{m} \quad (49)$$

$$X_Y = \frac{g_Y}{g_B} \quad \text{for } g_A \leq g_Y \leq g_{AB} \quad \text{if } C_{a2} = C_{\text{eff}} \text{ (see 14.3)} \quad (50)$$

$$X_Y = \frac{1}{3} + \frac{1}{3} \cdot \frac{g_Y}{g_B} \quad \text{for } g_{AB} \leq g_Y \leq g_B \quad \text{if } C_{a1} = 0 \mu\text{m} \quad (51)$$

$$X_Y = \frac{g_Y}{g_B} \quad \text{for } g_{AB} \leq g_Y \leq g_B \quad \text{if } C_{a1} = C_{\text{eff}} \quad (52)$$

$$X_Y = 1,0 \quad \text{for } g_B \leq g_Y \leq g_D \quad (53)$$

$$X_Y = \frac{1}{3} + \frac{1}{3} \cdot \frac{g_\alpha - g_Y}{g_\alpha - g_D} \quad \text{for } g_D \leq g_Y \leq g_{DE} \quad \text{if } C_{a2} = 0 \mu\text{m} \quad (54)$$

$$X_Y = \frac{g_\alpha - g_Y}{g_\alpha - g_D} \quad \text{for } g_D \leq g_Y \leq g_{DE} \quad \text{if } C_{a2} = C_{\text{eff}} \quad (55)$$

$$X_Y = \frac{1}{3} + \frac{1}{3} \cdot \frac{g_\alpha - g_Y}{g_\alpha - g_D} \quad \text{for } g_{DE} \leq g_Y \leq g_E \quad \text{if } C_{a1} = 0 \mu\text{m} \quad (56)$$

$$X_Y = \frac{g_\alpha - g_Y}{g_\alpha - g_D} \quad \text{for } g_{DE} \leq g_Y \leq g_E \quad \text{if } C_{a1} = C_{\text{eff}} \quad (57)$$

11.3 Buttressing factor $X_{\text{but},Y}$

Helical gears may have a buttressing effect near the end points A and E of the path of contact, due to the oblique contact lines. This applies to cylindrical helical gears with no profile modification.

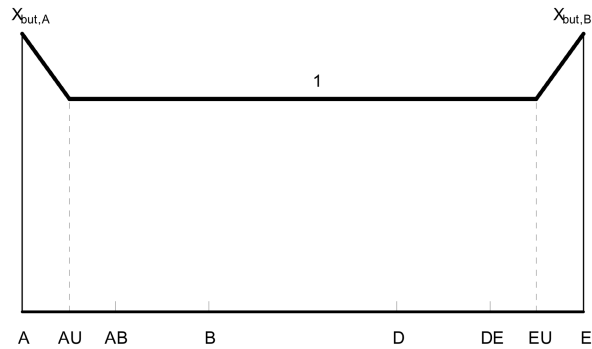


Figure 7 — Buttringing factor, $X_{but,Y}$

The buttringing is expressed by means of a factor $X_{but,Y}$; see Figure 7, marked by the following values.

$$g_{AU} - g_A = g_E - g_{EU} = 0,2 \text{ mm} \cdot \sin \beta_b \quad (58)$$

with

$$g_A = 0 \text{ mm} ;$$

$$g_E = g_\alpha \quad (\text{see Figure 1}).$$

$$X_{but,A} = X_{but,E} = 1,3 \quad \text{if } \varepsilon_\beta \geq 1,0 \quad (59)$$

$$X_{but,A} = X_{but,E} = 1 + 0,3 \cdot \varepsilon_\beta \quad \text{if } \varepsilon_\beta < 1,0 \quad (60)$$

$$X_{but,AU} = X_{but,EU} = 1,0 \quad (61)$$

$$X_{but,Y} = X_{but,A} - \frac{g_Y}{0,2 \text{ mm} \cdot \sin \beta_b} \cdot (X_{but,A} - 1) \quad \text{for } g_A \leq g_Y < g_{AU} \quad (62)$$

$$X_{but,Y} = 1,0 \quad \text{for } g_{AU} \leq g_Y \leq g_{EU} \quad (63)$$

$$X_{but,Y} = X_{but,E} - \frac{g_\alpha - g_Y}{0,2 \text{ mm} \cdot \sin \beta_b} \cdot (X_{but,E} - 1) \quad \text{for } g_{EU} < g_Y \leq g_E \quad (64)$$

where

ε_β is the overlap ratio.

11.4 Helical gears with $\varepsilon_\beta < 1$ and unmodified profiles

Helical gears with a contact ratio $\varepsilon_\alpha \geq 1$ and overlap ratio $\varepsilon_\beta < 1$, have still poor single contact of tooth pairs. Hence, they can be treated similar to spur gears, considering the geometry in the transverse plane, as well as the buttringing effect. See Figure 8.

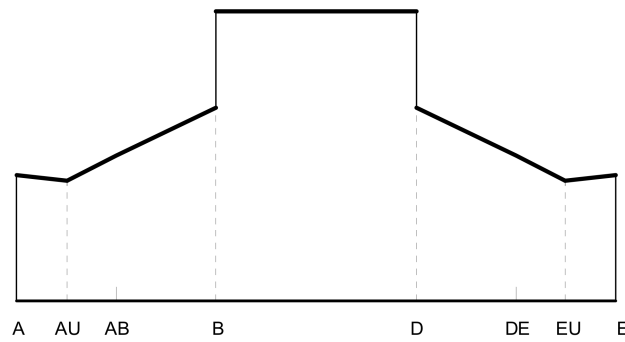


Figure 8 — Load sharing factor for cylindrical helical gears with $\epsilon_\beta < 1$ and unmodified profiles, including the buttressing effect

The load sharing factor is obtained by multiplying the X_Y in 11.1 with the buttressing factor $X_{but,Y}$ in 11.3.

11.5 Helical gears with $\epsilon_\beta < 1$ and profile modification

Helical gears with a contact ratio $\epsilon_\alpha \geq 1$ and overlap ratio $\epsilon_\beta < 1$, have still poor single contact of tooth pairs. Hence, they can be treated similar to spur gears, considering the geometry in the transverse plane. See Figure 9, Figure 10 and Figure 11.

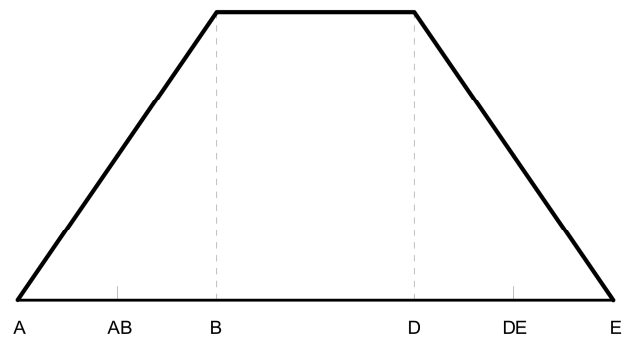


Figure 9 — Load sharing factor for cylindrical helical gears with $\epsilon_\beta < 1$ and optimum profile modification

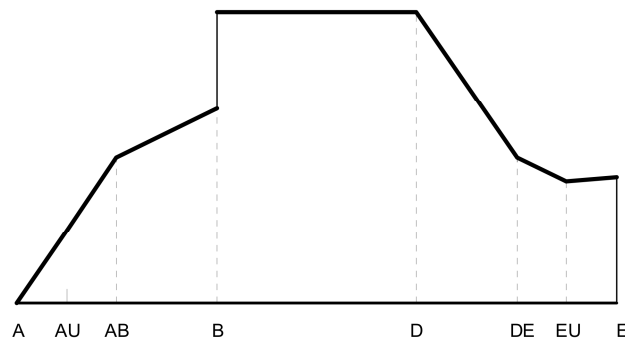


Figure 10 — Load sharing factor for cylindrical helical gears with $\epsilon_\beta < 1$ and optimum profile modification on the addendum of the driven gear and/or the dedendum of the driving gear

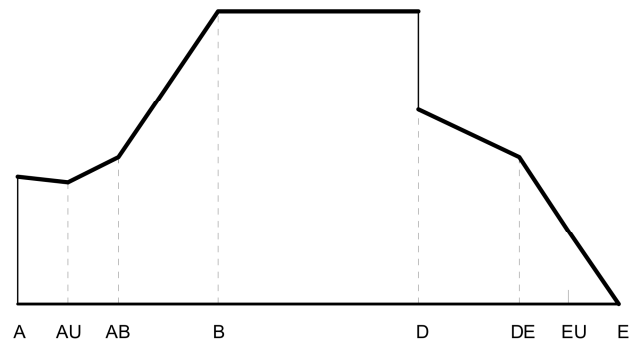


Figure 11 — Load sharing factor for cylindrical helical gears with $\varepsilon_{\beta} < 1$ and optimum profile modification on the addendum of the driving gear and/or the dedendum of the driven gear

The load sharing factor is obtained by multiplying the X_Y in 11.2 with the buttressing factor $X_{but,Y}$ in 11.3.

11.6 Helical gears with $\varepsilon_{\beta} \geq 1$ and unmodified profiles

The buttressing effect of local high mesh stiffness at the end of oblique contact lines for helical gears with $\varepsilon_{\alpha} \geq 1$ and $\varepsilon_{\beta} \geq 1$, is assumed to act near the ends A and E along the helix teeth over a constant length, which corresponds to a transverse relative distance $0,2 \text{ mm} \cdot \sin \beta_b$; see Figure 12. See also 11.3 and Figure 7.

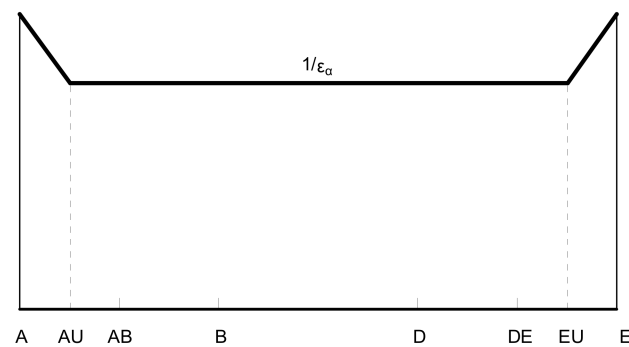


Figure 12 — Load sharing factor for cylindrical helical gears with $\varepsilon_{\beta} \geq 1$ and unmodified profiles

The load sharing factor is obtained by multiplying the value $1/\varepsilon_{\alpha}$, representing the mean load, with the buttressing factor $X_{but,Y}$.

$$X_Y = \frac{1}{\varepsilon_{\alpha}} \cdot X_{but,Y} \quad (65)$$

where

ε_{α} is the transverse contact ratio.

11.7 Helical gears with $\epsilon_{\beta} \geq 1$ and profile modification

Tip relief on the pinion (respectively wheel) reduces X_{γ} in the range DE-E (respectively A-AB) and increases X_{γ} in the range AB-DE, see Figure 13, Figure 14 and Figure 15. The extensions of tip relief at both ends A-AB and DE-E of the path of contact are assumed to be equal and to result in a contact ratio $\epsilon_{\alpha} = 1$ for unloaded gears; see Figure 13.

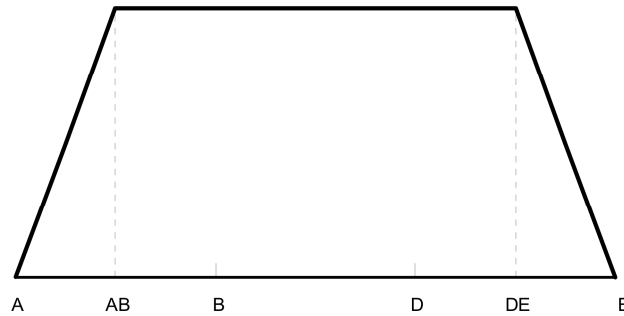


Figure 13 — Load sharing factor for cylindrical helical gears with $\epsilon_{\beta} \geq 1$ and optimum profile modification



Figure 14 — Load sharing factor for cylindrical helical gears with $\epsilon_{\beta} \geq 1$ and optimum profile modification on the addendum of the driven gear and/or the dedendum of the driving gear



Figure 15 — Load sharing factor for cylindrical helical gears with $\epsilon_{\beta} \geq 1$ and optimum profile modification on the addendum of the driving gear and/or the dedendum of the driven gear

The ranges are marked by the following values. Linear interpolation between these values is possible.

$$X_Y = \left[\frac{1}{\varepsilon_\alpha} + \frac{(\varepsilon_\alpha - 1)}{2 \cdot \varepsilon_\alpha \cdot (\varepsilon_\alpha + 1)} \right] \cdot X_{\text{but},Y} \quad \text{for } g_A \leq g_Y \leq g_{AB} \quad \text{if } C_{a1} = C_{\text{eff}} \text{ and } C_{a2} = 0 \mu\text{m} \quad (66)$$

$$X_Y = \left[\frac{1}{\varepsilon_\alpha} + \frac{(\varepsilon_\alpha - 1)}{2 \cdot \varepsilon_\alpha \cdot (\varepsilon_\alpha + 1)} \right] \cdot \frac{g_Y}{g_{AB}} \quad \text{for } g_A \leq g_Y \leq g_{AB} \quad \text{if } C_{a1} = 0 \mu\text{m} \text{ and } C_{a2} = C_{\text{eff}} \quad (67)$$

$$X_Y = \left[\frac{1}{\varepsilon_\alpha} + \frac{(\varepsilon_\alpha - 1)}{\varepsilon_\alpha \cdot (\varepsilon_\alpha + 1)} \right] \cdot \frac{g_Y}{g_{AB}} \quad \text{for } g_A \leq g_Y \leq g_{AB} \quad \text{if } C_{a1} = C_{a2} = C_{\text{eff}} \quad (68)$$

$$X_Y = \frac{1}{\varepsilon_\alpha} + \frac{(\varepsilon_\alpha - 1)}{2 \cdot \varepsilon_\alpha \cdot (\varepsilon_\alpha + 1)} \quad \text{for } g_{AB} \leq g_Y \leq g_{DE} \quad \text{if } C_{a1} = 0 \mu\text{m} \text{ and } C_{a2} = C_{\text{eff}} \quad (69)$$

if $C_{a1} = C_{\text{eff}}$ and $C_{a2} = 0 \mu\text{m}$

$$X_Y = \frac{1}{\varepsilon_\alpha} + \frac{(\varepsilon_\alpha - 1)}{\varepsilon_\alpha \cdot (\varepsilon_\alpha + 1)} \quad \text{for } g_{AB} \leq g_Y \leq g_{DE} \quad \text{if } C_{a1} = C_{a2} = C_{\text{eff}} \quad (70)$$

$$X_Y = \left[\frac{1}{\varepsilon_\alpha} + \frac{(\varepsilon_\alpha - 1)}{2 \cdot \varepsilon_\alpha \cdot (\varepsilon_\alpha + 1)} \right] \cdot \frac{g_\alpha - g_Y}{g_\alpha - g_{DE}} \quad \text{for } g_{DE} \leq g_Y \leq g_E \quad \text{if } C_{a1} = C_{\text{eff}} \text{ and } C_{a2} = 0 \mu\text{m} \quad (71)$$

$$X_Y = \left[\frac{1}{\varepsilon_\alpha} + \frac{(\varepsilon_\alpha - 1)}{2 \cdot \varepsilon_\alpha \cdot (\varepsilon_\alpha + 1)} \right] \cdot X_{\text{but},Y} \quad \text{for } g_{DE} \leq g_Y \leq g_E \quad \text{if } C_{a1} = 0 \mu\text{m} \text{ and } C_{a2} = C_{\text{eff}} \quad (72)$$

$$X_Y = \left[\frac{1}{\varepsilon_\alpha} + \frac{(\varepsilon_\alpha - 1)}{\varepsilon_\alpha \cdot (\varepsilon_\alpha + 1)} \right] \cdot \frac{g_\alpha - g_Y}{g_\alpha - g_{DE}} \quad \text{for } g_{DE} \leq g_Y \leq g_E \quad \text{if } C_{a1} = C_{a2} = C_{\text{eff}} \quad (73)$$

12 Contact temperature $\theta_{B,Y}$

The local contact temperature $\theta_{B,Y}$ is defined as the sum of bulk temperature θ_M and local flash temperature $\theta_{fl,Y}$. As a result of friction in the teeth mesh, the flash temperature $\theta_{fl,Y}$ varies along the path of contact. Hence the local flash temperature $\theta_{fl,Y}$ has to be determined for every desired point Y in the field of contact. For simplification the bulk temperature θ_M is assumed as constant.

$$\theta_{B,Y} = \theta_M + \theta_{fl,Y} \quad (74)$$

where

$\theta_{fl,Y}$ is the local flash temperature (see clause 13);

θ_M is the bulk temperature (see clause 14).

13 Flash temperature $\theta_{fl,Y}$

The flash temperature $\theta_{fl,Y}$ of the gear flanks is rapidly fluctuating in contact. In every mesh position different rolling and sliding conditions occur. Furthermore the local contact load varies along the path of contact. These conditions cause a continuous variation of the flash temperature which can be calculated according to Blok [13] by equation (75).

$$\theta_{fl,Y} = \frac{\sqrt{\pi}}{2} \cdot \frac{\mu_m \cdot \rho_{dyn,Y} \cdot 10^6 \cdot |V_{g,Y}|}{B_{M1} \cdot \sqrt{V_{r1,Y}} + B_{M2} \cdot \sqrt{V_{r2,Y}}} \cdot \sqrt{8 \cdot \rho_{n,Y} \cdot \frac{\rho_{dyn,Y}}{1000 \cdot E_r}} \quad (75)$$

where

$$V_{g,Y} = V_{r1,Y} - V_{r2,Y} \quad (76)$$

$$B_{M1} = \sqrt{\rho_{M1} \cdot c_{M1} \cdot \lambda_{M1}} \quad (77)$$

$$B_{M2} = \sqrt{\rho_{M2} \cdot c_{M2} \cdot \lambda_{M2}} \quad (78)$$

- $V_{g,Y}$ is the local sliding velocity;
- B_{M1} is the thermal contact coefficient of pinion (see Table 2);
- B_{M2} is the thermal contact coefficient of wheel (see Table 2);
- μ_m is the mean coefficient of friction (see 14.1);
- $\rho_{dyn,Y}$ is the local Hertzian contact stress (see 8.1 and 8.2);
- $V_{r1,Y}$ is the local tangential velocity on pinion (see 7.1);
- $V_{r2,Y}$ is the local tangential velocity on wheel (see 7.1);
- $\rho_{n,Y}$ is the local normal radius of relative curvature (see clause 10);
- E_r is the reduced modulus of elasticity (see 6.1).

Table 2 — Material properties of steel

material	density ρ_M [kg/m ³]	specific heat capacity c_M [J/(kg·K)]	specific heat conductivity λ_M [W/(m·K)]
steel	7800	440	45

14 Bulk temperature θ_M

The bulk temperature θ_M is the equilibrium temperature of the surface of the gear teeth before they enter the contact zone. The bulk temperature θ_M should be measured or calculated by an adequate method. If this is not possible θ_M can be approximated according to equation (79) (compare [10]).

$$\theta_M = \theta_{oil} + 7400 \cdot \left(\frac{P \cdot \mu_m \cdot H_v}{a \cdot b} \right)^{0,72} \cdot \frac{X_S}{1,2 \cdot X_{Ca}} \quad (79)$$

where

$$P = 2 \cdot \pi \cdot \frac{n_1}{60} \cdot \frac{T_1}{1000} \quad (80)$$

- P is the transmitted power;

- a is the centre distance;
- b is the face width;
- θ_{oil} is the lubricant inlet or oil sump temperature;
- μ_m is the mean coefficient of friction (see 14.1);
- H_v is the load losses factor (see 14.2);
- X_{Ca} is the tip relief factor (see 14.3);
- X_S is the lubricant factor (see 14.4).

14.1 Mean coefficient of friction μ_m

The mean coefficient of friction μ_m depends on the gear geometry, the surface roughness, the tangential velocity, the tangential load and the dynamic viscosity of the lubricant. It can be approximated by equation (81).

$$\mu_m = 0,045 \cdot \left(\frac{K_A \cdot K_V \cdot K_{H\alpha} \cdot K_{H\beta} \cdot F_{bt} \cdot K_{By}}{b \cdot v_{\Sigma,C} \cdot \rho_{n,C}} \right)^{0,2} \cdot (10^3 \cdot \eta_{\theta oil})^{-0,05} \cdot X_R \cdot X_L \quad (81)$$

where

$$X_R = 2,2 \cdot \left(\frac{Ra}{\rho_{n,C}} \right)^{0,25} \quad (82)$$

- X_R is the roughness factor;
- b is the face width;
- F_{bt} is the nominal transverse load in plane of action;
- K_A is the application factor (according to ISO 6336-1);
- K_{By} is the helical load factor (see below);
- $K_{H\alpha}$ is the transverse load factor (according to ISO 6336-1);
- $K_{H\beta}$ is the face load factor (according to ISO 6336-1);
- K_V is the dynamic factor (according to ISO 6336-1);
- $v_{\Sigma,C}$ is the sum of the tangential velocities at the pitch point (see 7.1);
- $\eta_{\theta oil}$ is the dynamic viscosity at inlet or oil sump temperature;
- $\rho_{n,C}$ is the normal radius of relative curvature at the pitch diameter;
- Ra is the effective arithmetic mean roughness value (see 5.3);
- X_L is the lubricant factor (see Table 3).

The helical load factor K_{By} takes into account an increasing friction for increasing total contact ratio (see Figure 16).

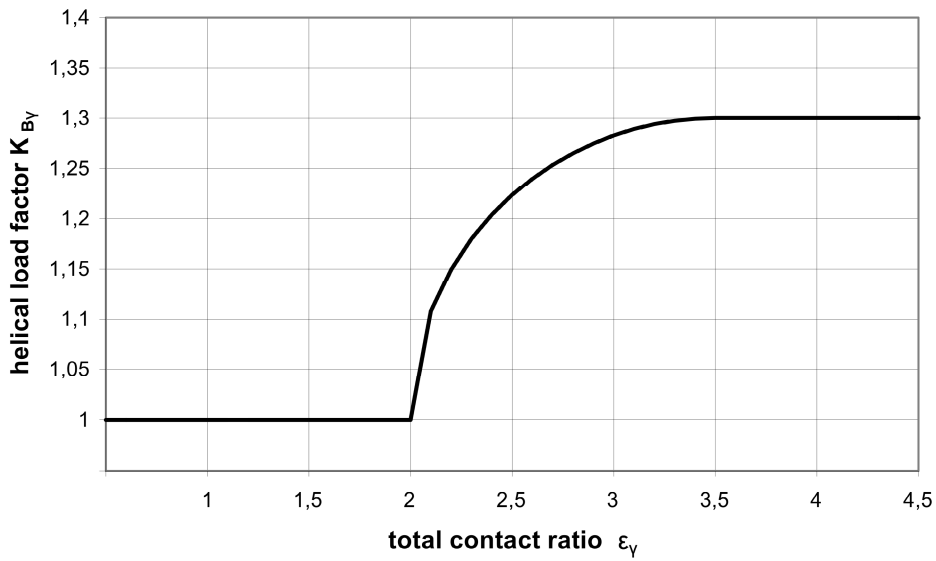


Figure 16 — Helical load factor K_{By}

$$K_{By} = 1,0 \quad \text{if } \epsilon_v \leq 2 \quad (83)$$

$$K_{By} = 1 + 0,2 \cdot \sqrt{(\epsilon_v - 2) \cdot (5 - \epsilon_v)} \quad \text{if } 2 < \epsilon_v < 3,5 \quad (84)$$

$$K_{By} = 1,3 \quad \text{if } \epsilon_v \geq 3,5 \quad (85)$$

Table 3 — Lubricant factor, X_L

oil type	X_L
mineral oil	1,0
polyalphaolefin	0,8
non water-soluble polyglycols	0,7
water-soluble polyglycols	0,6
traction fluid	1,5
phosphate ester	1,3

14.2 Load losses factor H_v

The load losses factor H_v is calculated according to equation (86) and (87).

$$H_v = (\epsilon_1^2 + \epsilon_2^2 + 1 - \epsilon_\alpha) \cdot \left(\frac{1}{z_1} + \frac{1}{z_2} \right) \cdot \frac{\pi}{\cos \beta_b} \quad \text{if } \epsilon_\alpha < 2 \quad (86)$$

$$H_v = 0,5 \cdot \varepsilon_\alpha \cdot \left(\frac{1}{z_1} + \frac{1}{z_2} \right) \cdot \frac{\pi}{\cos \beta_b} \quad \text{if } \varepsilon_\alpha \geq 2 \quad (87)$$

where

- z_1 is the number of teeth of pinion;
- z_2 is the number of teeth of wheel;
- β_b is the base helix angle;
- ε_1 is the addendum contact ratio of the pinion;
- ε_2 is the addendum contact ratio of the wheel;
- ε_α is the transverse contact ratio.

14.3 Tip relief factor X_{Ca}

The elastic deformation of the meshing teeth results in overload on the tip in the area of high sliding. The tip relief factor X_{Ca} according to Figure 17 considers the positive influence of the profile modification on this overload. X_{Ca} is a relative tip relief factor which depends on the actual values of tip relief C_{a1} , C_{a2} , the effective tip relief C_{eff} , the ratio of addendum contact ratios and the direction of power flow.

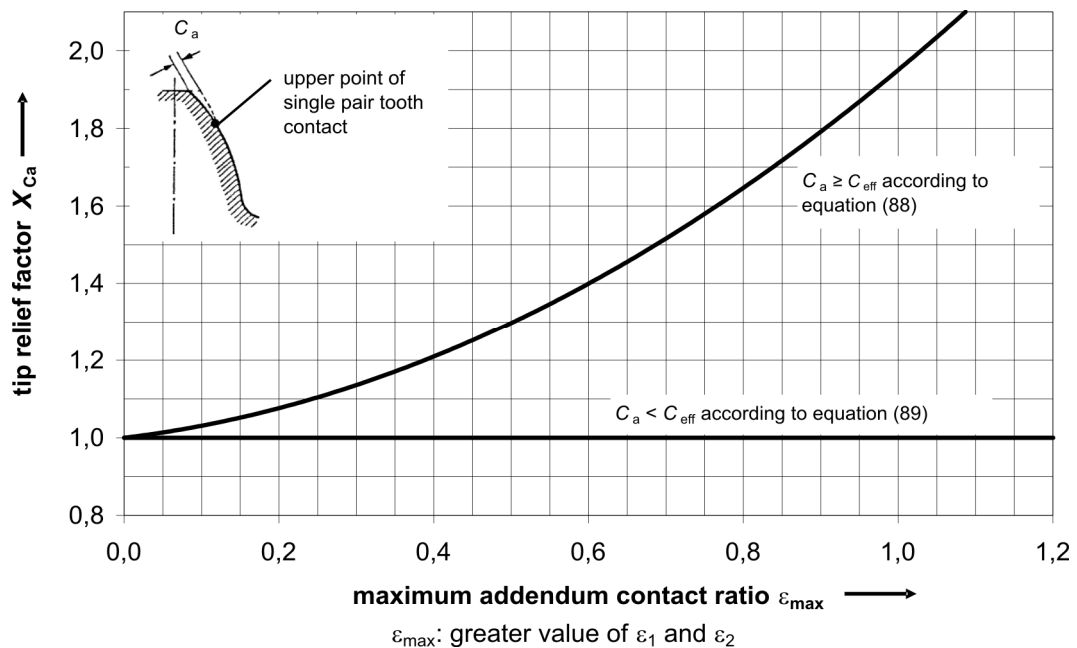


Figure 17 — Tip relief factor X_{Ca}

The curves in Figure 17 can be approximated by the following equations:

$$X_{Ca} = 1 + 0,24 \cdot \varepsilon_{max} + 0,71 \cdot \varepsilon_{max}^2 \quad (88)$$

- if pinion drives wheel and $\varepsilon_1 > 1,5 \cdot \varepsilon_2$ and $C_{a1} \geq C_{eff}$
- if pinion drives wheel and $\varepsilon_1 \leq 1,5 \cdot \varepsilon_2$ and $C_{a2} \geq C_{eff}$
- if wheel drives pinion and $\varepsilon_1 > (2/3) \cdot \varepsilon_2$ and $C_{a1} \geq C_{eff}$
- if wheel drives pinion and $\varepsilon_1 \leq (2/3) \cdot \varepsilon_2$ and $C_{a2} \geq C_{eff}$

$$X_{Ca} = 1,0 \quad \text{in all other cases} \quad (89)$$

where

C_{eff} is the effective tip relief (see below);

ε_{max} is the maximum value, ε_1 or ε_2 .

C_{eff} is the effective tip relief, that amount of tip relief which compensates for the elastic deformation of the teeth in single pair contact.

$$C_{eff} = \frac{K_A \cdot F_t}{b \cdot c'} \quad \text{for spur gears} \quad (90)$$

$$C_{eff} = \frac{K_A \cdot F_t}{b \cdot c_{\gamma\alpha}} \quad \text{for helical gears} \quad (91)$$

where

b is the face width;

c' is the single stiffness of a tooth pair per unit face width (according to ISO 6336-1);

$c_{\gamma\alpha}$ is the mean value of mesh stiffness per unit face width (according to ISO 6336-1);

F_t is the transverse tangential load at reference cylinder;

K_A is the application factor (according to ISO 6336-1).

Tip relief factor as described above applies to gears of ISO accuracy grade ≤ 6 , in accordance with ISO 1328-1. For less accurate gears, X_{Ca} is to be set equal to 1; see also ISO 6336-1.

14.4 Lubrication factor X_S

The lubrication factor takes into account a better heat transfer for dip lubrication than for injection lubrication. The following values apply.

$X_S = 1,2$ for injection lubrication;

$X_S = 1,0$ for dip lubrication;

$X_S = 0,2$ for gears submerged in oil.

Annex A (informative)

Calculation of the permissible specific lubricant film thickness λ_{GFP} for oils with a micropitting test result according to FVA-Information Sheet 54/7

The following information in this annex is provided as reference only and should not be interpreted as generalised part of the procedure defined in this Technical Report.

One test procedure used to evaluate the micropitting load capacity of gear lubricants is the FVA-FZG-micropitting test according to FVA-Information Sheet 54/7 [7].

For mineral oils investigated in this test procedure λ_{GFP} can be taken from Figure A.1 depending on the nominal oil viscosity and the failure load stage SKS reached in the test C-GF/8,3/90. Interpolation between the stated values is possible.

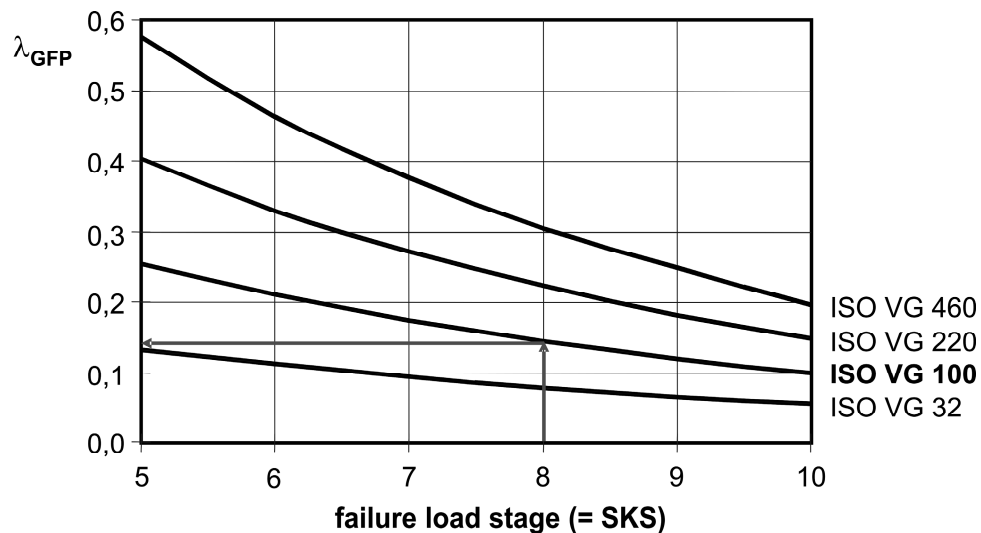


Figure A.1 — Minimum permissible specific lubricant film thickness for mineral oils as function of nominal lubricant viscosity and failure load stage SKS of the FVA-FZG micropitting test C-GF/8,3/90 with $R_a = 0,50 \mu\text{m}$

For other test conditions or different lubricants than presented in Figure A.1 the critical specific lubricant film thickness λ_{GFT} in contact point A of the specified test gears type C-GF is calculated at the reached failure load stage according to equation (2). The required gear geometry of the test gears type C-GF is specified in FVA-Information Sheet 54/7. In this case the permissible specific lubricant film thickness λ_{GFP} is defined according to equation (A.1). The material factor W_W takes into account the influence of gear material different from the case carburised standardised test gears type C-GF.

$$\lambda_{GFP} = 1,4 \cdot W_W \cdot \lambda_{GFT} \quad (\text{A.1})$$

where

W_W is the material factor (see Table A.1);

λ_{GFT} is the specific lubricant film thickness ascertained by tests (see 5.3).

NOTE If no value for the failure load stage SKS of the lubricant is available, use the value λ_{GFP} of the lubricant for failure load stage SKS 5.

Table A.1 — Material factor, W_w

Material	Material factor, W_w
Case carburised steel, with austenite content: - less than 25 % - greater than 25 %	1,0 0,95
Gas nitrided steel (HV > 850)	1,5
Induction, flame hardened steel	0,65
Through hardened steel	0,5

Annex B (informative)

Example calculation

In the following annex an example calculation is presented. The calculation sequence has been provided to follow a logical approach with relation to the input data.

The example calculates the safety factor S_λ of a specific gear set when compared to an allowable λ_{GFP} value. Whilst any suitable test method can be used to determine the allowable λ_{GFP} value the calculation provided uses a λ_{GFP} established by the FVA-FZG micropitting test (Method B) as outlined in Annex A.

The result of this example is confirmed by experimental investigations. The gears were obviously micropitted and had profile deviations of approximately 10 μm .

B.1 Input

B.1.1 Input of gear data

number of teeth of pinion:	$z_1 = 18$
number of teeth of wheel:	$z_2 = 18$
normal module:	$m_n = 10,93 \text{ mm}$
tip diameter of pinion:	$d_{a1} = 221,4 \text{ mm}$
tip diameter of wheel:	$d_{a2} = 221,4 \text{ mm}$
addendum modification factor of pinion:	$x_1 = 0,158$
addendum modification factor of wheel:	$x_2 = 0,158$
face width:	$b = 21,4 \text{ mm}$
helix angle:	$\beta = 0^\circ$
normal pressure angle:	$\alpha_n = 20^\circ$
centre distance:	$a = 200 \text{ mm}$
gear quality:	$Q = 5$
arithmetic mean roughness value of pinion:	$Ra_1 = 0,90 \mu\text{m}$
arithmetic mean roughness value of wheel:	$Ra_2 = 0,90 \mu\text{m}$
tooth flank modifications:	no modifications

B.1.2 Input of material data

modulus of elasticity of pinion:	$E_1 = 206000 \text{ N/mm}^2$
modulus of elasticity of wheel:	$E_2 = 206000 \text{ N/mm}^2$
Poisson's ratio of pinion:	$\nu_1 = 0,3$
Poisson's ratio of wheel:	$\nu_2 = 0,3$
specific heat conductivity of pinion:	$\lambda_{M1} = 45 \text{ W/(mK)}$
specific heat conductivity of wheel:	$\lambda_{M2} = 45 \text{ W/(mK)}$
specific heat per unit mass of pinion:	$c_{M1} = 440 \text{ J/(kgK)}$
specific heat per unit mass of wheel:	$c_{M2} = 440 \text{ J/(kgK)}$
density of pinion:	$\rho_{M1} = 7800 \text{ kg/m}^3$
density of wheel:	$\rho_{M2} = 7800 \text{ kg/m}^3$
material factor according to Table A.1: (for matching case carburised/ case carburised)	$W_W = 1,0$

B.1.3 Input of operating data

nominal torque at the pinion:	$T_1 = 1878 \text{ Nm}$
rotation speed of the pinion:	$n_1 = 3000 \text{ min}^{-1}$
application factor:	$K_A = 1,0$
dynamic factor:	$K_V = 1,15$
transverse load factor:	$K_{H\alpha} = 1,0$
face load factor:	$K_{H\beta} = 1,10$

B.1.4 Input of lubricant data

oil inlet temperature (injection lubrication):	$\theta_{oil} = 90 \text{ }^\circ\text{C}$
kinematic viscosity at 40 °C:	$\nu_{40} = 210 \text{ mm}^2/\text{s}$
kinematic viscosity at 100 °C:	$\nu_{100} = 18,5 \text{ mm}^2/\text{s}$
density of the lubricant at 15 °C:	$\rho_{15} = 895 \text{ kg/m}^3$
oil type:	mineral oil
failure load stage at operating temperature according to FVA 54/7:	SKS 8

B.2 Calculation of the current specific lubricant film thickness

B.2.1 Calculation of gear geometry (according to ISO 21771)

basic values:

$$m_t = \frac{m_n}{\cos \beta} \quad m_t = 10,93 \text{ mm}$$

$$d_1 = z_1 \cdot m_t \quad d_1 = 196,74 \text{ mm}$$

$$d_2 = z_2 \cdot m_t \quad d_2 = 196,74 \text{ mm}$$

$$u = \frac{z_2}{z_1} \quad u = 1$$

$$\alpha_t = \arctan\left(\frac{\tan \alpha_n}{\cos \beta}\right) \quad \alpha_t = 20^\circ$$

$$d_{b1} = d_1 \cdot \cos \alpha_t \quad d_{b1} = 184,875 \text{ mm}$$

$$d_{b2} = d_2 \cdot \cos \alpha_t \quad d_{b2} = 184,875 \text{ mm}$$

$$d_{w1} = \frac{2 \cdot a}{u + 1} \quad d_{w1} = 200 \text{ mm}$$

$$d_{w2} = 2 \cdot a - d_{w1} \quad d_{w2} = 200 \text{ mm}$$

$$\alpha_{wt} = \arccos\left[\frac{(z_1 + z_2) \cdot m_t \cdot \cos \alpha_t}{2 \cdot a}\right] \quad \alpha_{wt} = 22,426^\circ$$

$$\beta_b = \arcsin(\sin \beta \cdot \cos \alpha_n) \quad \beta_b = 0^\circ$$

$$\rho_{et} = m_t \cdot \pi \cdot \cos \alpha_t \quad \rho_{et} = 32,267 \text{ mm}$$

$$\varepsilon_1 = \frac{z_1}{2 \cdot \pi} \cdot \left[\sqrt{\left(\frac{d_{a1}}{d_{b1}}\right)^2} - 1 - \tan \alpha_{wt} \right] \quad \varepsilon_1 = 0,705$$

$$\varepsilon_2 = \frac{z_2}{2 \cdot \pi} \cdot \left[\sqrt{\left(\frac{d_{a2}}{d_{b2}}\right)^2} - 1 - \tan \alpha_{wt} \right] \quad \varepsilon_2 = 0,705$$

$$\varepsilon_\alpha = \frac{1}{\rho_{et}} \cdot \left(\sqrt{\frac{d_{a1}^2}{4} - \frac{d_{b1}^2}{4}} + \sqrt{\frac{d_{a2}^2}{4} - \frac{d_{b2}^2}{4}} - a \cdot \sin \alpha_{wt} \right) \quad \varepsilon_\alpha = 1,411$$

$$\varepsilon_\beta = \frac{b \cdot \sin \beta}{m_n \cdot \pi} \quad \varepsilon_\beta = 0$$

$$\varepsilon_Y = \varepsilon_\alpha + \varepsilon_\beta$$

$$\varepsilon_\gamma = 1,411$$

$$g_\alpha = 0,5 \cdot \left(\sqrt{d_{a1}^2 - d_{b1}^2} + \sqrt{d_{a2}^2 - d_{b2}^2} \right) - a \cdot \sin \alpha_{wt}$$

$$g_\alpha = 45,519 \text{ mm}$$

coordinates of the basic points (A, AB, B, C, D, DE, E) on the line of action (see clause 10):

$$g_A = 0 \text{ mm}$$

$$g_A = 0 \text{ mm}$$

$$g_{AB} = \frac{g_\alpha - p_{et}}{2}$$

$$g_{AB} = 6,626 \text{ mm}$$

$$g_B = g_\alpha - p_{et}$$

$$g_B = 13,253 \text{ mm}$$

$$g_C = \frac{d_{b1}}{2} \cdot \tan \alpha_{wt} - \sqrt{\frac{d_{a1}^2}{4} - \frac{d_{b1}^2}{4}} + g_\alpha$$

$$g_C = 22,760 \text{ mm}$$

$$g_D = p_{et}$$

$$g_D = 32,267 \text{ mm}$$

$$g_{DE} = \frac{g_\alpha - p_{et}}{2} + p_{et}$$

$$g_{DE} = 38,893 \text{ mm}$$

$$g_E = g_\alpha$$

$$g_E = 45,519 \text{ mm}$$

$$d_{A1} = 2 \cdot \sqrt{\frac{d_{b1}^2}{4} + \left(\sqrt{\frac{d_{a1}^2}{4} - \frac{d_{b1}^2}{4}} - g_\alpha + g_A \right)^2}$$

$$d_{A1} = 187,419 \text{ mm}$$

$$d_{AB1} = 2 \cdot \sqrt{\frac{d_{b1}^2}{4} + \left(\sqrt{\frac{d_{a1}^2}{4} - \frac{d_{b1}^2}{4}} - g_\alpha + g_{AB} \right)^2}$$

$$d_{AB1} = 190,046 \text{ mm}$$

$$d_{B1} = 2 \cdot \sqrt{\frac{d_{b1}^2}{4} + \left(\sqrt{\frac{d_{a1}^2}{4} - \frac{d_{b1}^2}{4}} - g_\alpha + g_B \right)^2}$$

$$d_{B1} = 193,546 \text{ mm}$$

$$d_{C1} = 2 \cdot \sqrt{\frac{d_{b1}^2}{4} + \left(\sqrt{\frac{d_{a1}^2}{4} - \frac{d_{b1}^2}{4}} - g_\alpha + g_C \right)^2}$$

$$d_{C1} = 200,000 \text{ mm}$$

$$d_{D1} = 2 \cdot \sqrt{\frac{d_{b1}^2}{4} + \left(\sqrt{\frac{d_{a1}^2}{4} - \frac{d_{b1}^2}{4}} - g_\alpha + g_D \right)^2}$$

$$d_{D1} = 207,998 \text{ mm}$$

$$d_{DE1} = 2 \cdot \sqrt{\frac{d_{b1}^2}{4} + \left(\sqrt{\frac{d_{a1}^2}{4} - \frac{d_{b1}^2}{4}} - g_\alpha + g_{DE} \right)^2}$$

$$d_{DE1} = 214,394 \text{ mm}$$

$$d_{E1} = 2 \cdot \sqrt{\frac{d_{b1}^2}{4} + \left(\sqrt{\frac{d_{a1}^2}{4} - \frac{d_{b1}^2}{4}} - g_a + g_E \right)^2} \quad d_{E1} = 221,400 \text{ mm}$$

$$d_{A2} = 2 \cdot \sqrt{\frac{d_{b2}^2}{4} + \left(\sqrt{\frac{d_{a2}^2}{4} - \frac{d_{b2}^2}{4}} - g_A \right)^2} \quad d_{A2} = 221,400 \text{ mm}$$

$$d_{AB2} = 2 \cdot \sqrt{\frac{d_{b2}^2}{4} + \left(\sqrt{\frac{d_{a2}^2}{4} - \frac{d_{b2}^2}{4}} - g_{AB} \right)^2} \quad d_{AB2} = 214,394 \text{ mm}$$

$$d_{B2} = 2 \cdot \sqrt{\frac{d_{b2}^2}{4} + \left(\sqrt{\frac{d_{a2}^2}{4} - \frac{d_{b2}^2}{4}} - g_B \right)^2} \quad d_{B2} = 207,998 \text{ mm}$$

$$d_{C2} = 2 \cdot \sqrt{\frac{d_{b2}^2}{4} + \left(\sqrt{\frac{d_{a2}^2}{4} - \frac{d_{b2}^2}{4}} - g_C \right)^2} \quad d_{C2} = 200,000 \text{ mm}$$

$$d_{D2} = 2 \cdot \sqrt{\frac{d_{b2}^2}{4} + \left(\sqrt{\frac{d_{a2}^2}{4} - \frac{d_{b2}^2}{4}} - g_D \right)^2} \quad d_{D2} = 193,546 \text{ mm}$$

$$d_{DE2} = 2 \cdot \sqrt{\frac{d_{b2}^2}{4} + \left(\sqrt{\frac{d_{a2}^2}{4} - \frac{d_{b2}^2}{4}} - g_{DE} \right)^2} \quad d_{DE2} = 190,046 \text{ mm}$$

$$d_{E2} = 2 \cdot \sqrt{\frac{d_{b2}^2}{4} + \left(\sqrt{\frac{d_{a2}^2}{4} - \frac{d_{b2}^2}{4}} - g_E \right)^2} \quad d_{E2} = 187,419 \text{ mm}$$

transverse radius of relative curvature:

$$\rho_{t1,A} = \sqrt{\frac{d_{A1}^2 - d_{b1}^2}{4}} \quad \rho_{t1,A} = 15,389 \text{ mm}$$

$$\rho_{t1,AB} = \sqrt{\frac{d_{AB1}^2 - d_{b1}^2}{4}} \quad \rho_{t1,AB} = 22,015 \text{ mm}$$

$$\rho_{t1,B} = \sqrt{\frac{d_{B1}^2 - d_{b1}^2}{4}} \quad \rho_{t1,B} = 28,641 \text{ mm}$$

$$\rho_{t1,C} = \sqrt{\frac{d_{C1}^2 - d_{b1}^2}{4}} \quad \rho_{t1,C} = 38,148 \text{ mm}$$

$$\rho_{t1,D} = \sqrt{\frac{d_{D1}^2 - d_{b1}^2}{4}}$$

$$\rho_{1,D} = 47,655 \text{ mm}$$

$$\rho_{t1,DE} = \sqrt{\frac{d_{DE1}^2 - d_{b1}^2}{4}}$$

$$\rho_{1,DE} = 54,282 \text{ mm}$$

$$\rho_{t1,E} = \sqrt{\frac{d_{E1}^2 - d_{b1}^2}{4}}$$

$$\rho_{1,E} = 60,908 \text{ mm}$$

$$\rho_{t2,A} = \sqrt{\frac{d_{A2}^2 - d_{b2}^2}{4}}$$

$$\rho_{2,A} = 60,908 \text{ mm}$$

$$\rho_{t2,AB} = \sqrt{\frac{d_{AB2}^2 - d_{b2}^2}{4}}$$

$$\rho_{2,AB} = 54,282 \text{ mm}$$

$$\rho_{t2,B} = \sqrt{\frac{d_{B2}^2 - d_{b2}^2}{4}}$$

$$\rho_{2,B} = 47,655 \text{ mm}$$

$$\rho_{t2,C} = \sqrt{\frac{d_{C2}^2 - d_{b2}^2}{4}}$$

$$\rho_{2,C} = 38,148 \text{ mm}$$

$$\rho_{t2,D} = \sqrt{\frac{d_{D2}^2 - d_{b2}^2}{4}}$$

$$\rho_{2,D} = 28,641 \text{ mm}$$

$$\rho_{t2,DE} = \sqrt{\frac{d_{DE2}^2 - d_{b2}^2}{4}}$$

$$\rho_{2,DE} = 22,015 \text{ mm}$$

$$\rho_{t2,E} = \sqrt{\frac{d_{E2}^2 - d_{b2}^2}{4}}$$

$$\rho_{2,E} = 15,389 \text{ mm}$$

$$\rho_{t,A} = \frac{\rho_{t1,A} \cdot \rho_{t2,A}}{\rho_{t1,A} + \rho_{t2,A}}$$

$$\rho_{t,A} = 12,285 \text{ mm}$$

$$\rho_{t,AB} = \frac{\rho_{t1,AB} \cdot \rho_{t2,AB}}{\rho_{t1,AB} + \rho_{t2,AB}}$$

$$\rho_{t,AB} = 15,663 \text{ mm}$$

$$\rho_{t,B} = \frac{\rho_{t1,B} \cdot \rho_{t2,B}}{\rho_{t1,B} + \rho_{t2,B}}$$

$$\rho_{t,B} = 17,890 \text{ mm}$$

$$\rho_{t,C} = \frac{\rho_{t1,C} \cdot \rho_{t2,C}}{\rho_{t1,C} + \rho_{t2,C}}$$

$$\rho_{t,C} = 19,074 \text{ mm}$$

$$\rho_{t,D} = \frac{\rho_{t1,D} \cdot \rho_{t2,D}}{\rho_{t1,D} + \rho_{t2,D}}$$

$$\rho_{t,D} = 17,890 \text{ mm}$$

$$\rho_{t,DE} = \frac{\rho_{t1,DE} \cdot \rho_{t2,DE}}{\rho_{t1,DE} + \rho_{t2,DE}}$$

$$\rho_{t,DE} = 15,663 \text{ mm}$$

$$\rho_{t,E} = \frac{\rho_{t1,E} \cdot \rho_{t2,E}}{\rho_{t1,E} + \rho_{t2,E}}$$

$$\rho_{t,E} = 12,285 \text{ mm}$$

normal radius of relative curvature:

$$\rho_{n,A} = \frac{\rho_{t,A}}{\cos \beta_b}$$

$$\rho_{n,A} = 12,285 \text{ mm}$$

$$\rho_{n,AB} = \frac{\rho_{t,AB}}{\cos \beta_b}$$

$$\rho_{n,AB} = 15,663 \text{ mm}$$

$$\rho_{n,B} = \frac{\rho_{t,B}}{\cos \beta_b}$$

$$\rho_{n,B} = 17,890 \text{ mm}$$

$$\rho_{n,C} = \frac{\rho_{t,C}}{\cos \beta_b}$$

$$\rho_{n,C} = 19,074 \text{ mm}$$

$$\rho_{n,D} = \frac{\rho_{t,D}}{\cos \beta_b}$$

$$\rho_{n,D} = 17,890 \text{ mm}$$

$$\rho_{n,DE} = \frac{\rho_{t,DE}}{\cos \beta_b}$$

$$\rho_{n,DE} = 15,663 \text{ mm}$$

$$\rho_{n,E} = \frac{\rho_{t,E}}{\cos \beta_b}$$

$$\rho_{n,E} = 12,285 \text{ mm}$$

B.2.2 Calculation of material data

$$E_r = 2 \cdot \left(\frac{1 - \nu_1^2}{E_1} + \frac{1 - \nu_2^2}{E_2} \right)^{-1}$$

$$E_r = 226374 \text{ N/mm}^2$$

$$B_{M1} = \sqrt{\lambda_{M1} \cdot \rho_{M1} \cdot c_{M1}}$$

$$B_{M1} = 12427,4 \text{ N/(ms}^{0,5}\text{K)}$$

$$B_{M2} = \sqrt{\lambda_{M2} \cdot \rho_{M2} \cdot c_{M2}}$$

$$B_{M2} = 12427,4 \text{ N/(ms}^{0,5}\text{K)}$$

B.2.3 Calculation of operating conditions

loading:

$$P = 2 \cdot \pi \cdot \frac{n_1}{60} \cdot \frac{T_1}{1000}$$

$$P = 590 \text{ kW}$$

$$F_t = 2000 \cdot \frac{T_1}{d_1}$$

$$F_t = 19091 \text{ N}$$

$$F_{bt} = 2000 \cdot \frac{T_1}{d_{b1}}$$

$$F_{bt} = 20316 \text{ N}$$

local load sharing factor:

(no tooth flank modification, spur gears, gear quality $\leq 7 \rightarrow$ see Figure 2)

$$X_A = \frac{1}{3} + \frac{1}{3} \cdot \frac{g_A}{g_B}$$

$$X_A = 0,333$$

$$X_{AB} = \frac{1}{3} + \frac{1}{3} \cdot \frac{g_{AB}}{g_B}$$

$$X_{AB} = 0,5$$

$$X_B = 1,0$$

$$X_B = 1,0$$

$$X_C = 1,0$$

$$X_C = 1,0$$

$$X_D = 1,0$$

$$X_D = 1,0$$

$$X_{DE} = \frac{1}{3} + \frac{1}{3} \cdot \frac{g_\alpha - g_{DE}}{g_\alpha - g_D}$$

$$X_{DE} = 0,5$$

$$X_E = \frac{1}{3} + \frac{1}{3} \cdot \frac{g_\alpha - g_E}{g_\alpha - g_D}$$

$$X_E = 0,333$$

elasticity factor:

$$Z_E = \sqrt{\frac{E_r}{2 \cdot \pi}}$$

$$Z_E = 189,812 \text{ (N/mm}^2\text{)}^{0,5}$$

local Hertzian contact stress:

$$\rho_{H,A,B} = Z_E \cdot \sqrt{\frac{F_t \cdot X_A}{b \cdot \rho_{n,A} \cdot \cos \alpha_t \cdot \cos \beta_b}}$$

$$\rho_{H,A,B} = 963 \text{ N/mm}^2$$

$$\rho_{H,AB,B} = Z_E \cdot \sqrt{\frac{F_t \cdot X_{AB}}{b \cdot \rho_{n,AB} \cdot \cos \alpha_t \cdot \cos \beta_b}}$$

$$\rho_{H,AB,B} = 1045 \text{ N/mm}^2$$

$$\rho_{H,B,B} = Z_E \cdot \sqrt{\frac{F_t \cdot X_B}{b \cdot \rho_{n,B} \cdot \cos \alpha_t \cdot \cos \beta_b}}$$

$$\rho_{H,B,B} = 1383 \text{ N/mm}^2$$

$$\rho_{H,C,B} = Z_E \cdot \sqrt{\frac{F_t \cdot X_C}{b \cdot \rho_{n,C} \cdot \cos \alpha_t \cdot \cos \beta_b}}$$

$$\rho_{H,C,B} = 1339 \text{ N/mm}^2$$

$$\rho_{H,D,B} = Z_E \cdot \sqrt{\frac{F_t \cdot X_D}{b \cdot \rho_{n,D} \cdot \cos \alpha_t \cdot \cos \beta_b}} \quad \rho_{H,D,B} = 1383 \text{ N/mm}^2$$

$$\rho_{H,DE,B} = Z_E \cdot \sqrt{\frac{F_t \cdot X_{DE}}{b \cdot \rho_{n,DE} \cdot \cos \alpha_t \cdot \cos \beta_b}} \quad \rho_{H,DE,B} = 1045 \text{ N/mm}^2$$

$$\rho_{H,E,B} = Z_E \cdot \sqrt{\frac{F_t \cdot X_E}{b \cdot \rho_{n,E} \cdot \cos \alpha_t \cdot \cos \beta_b}} \quad \rho_{H,E,B} = 963 \text{ N/mm}^2$$

$$\rho_{\text{dyn},A,B} = \rho_{H,A,B} \cdot \sqrt{K_A \cdot K_V \cdot K_{H\alpha} \cdot K_{H\beta}} \quad \rho_{\text{dyn},A,B} = 1084 \text{ N/mm}^2$$

$$\rho_{\text{dyn},AB,B} = \rho_{H,AB,B} \cdot \sqrt{K_A \cdot K_V \cdot K_{H\alpha} \cdot K_{H\beta}} \quad \rho_{\text{dyn},AB,B} = 1175 \text{ N/mm}^2$$

$$\rho_{\text{dyn},B,B} = \rho_{H,B,B} \cdot \sqrt{K_A \cdot K_V \cdot K_{H\alpha} \cdot K_{H\beta}} \quad \rho_{\text{dyn},B,B} = 1555 \text{ N/mm}^2$$

$$\rho_{\text{dyn},C,B} = \rho_{H,C,B} \cdot \sqrt{K_A \cdot K_V \cdot K_{H\alpha} \cdot K_{H\beta}} \quad \rho_{\text{dyn},C,B} = 1506 \text{ N/mm}^2$$

$$\rho_{\text{dyn},D,B} = \rho_{H,D,B} \cdot \sqrt{K_A \cdot K_V \cdot K_{H\alpha} \cdot K_{H\beta}} \quad \rho_{\text{dyn},D,B} = 1555 \text{ N/mm}^2$$

$$\rho_{\text{dyn},DE,B} = \rho_{H,DE,B} \cdot \sqrt{K_A \cdot K_V \cdot K_{H\alpha} \cdot K_{H\beta}} \quad \rho_{\text{dyn},DE,B} = 1175 \text{ N/mm}^2$$

$$\rho_{\text{dyn},E,B} = \rho_{H,E,B} \cdot \sqrt{K_A \cdot K_V \cdot K_{H\alpha} \cdot K_{H\beta}} \quad \rho_{\text{dyn},E,B} = 1084 \text{ N/mm}^2$$

velocity:

$$v_{r1,A} = 2 \cdot \pi \cdot \frac{n_1}{60} \cdot \frac{d_{w1}}{2000} \cdot \sin \alpha_{wt} \cdot \sqrt{\frac{d_{A1}^2 - d_{b1}^2}{d_{w1}^2 - d_{b1}^2}} \quad v_{r1,A} = 4,834 \text{ m/s}$$

$$v_{r1,AB} = 2 \cdot \pi \cdot \frac{n_1}{60} \cdot \frac{d_{w1}}{2000} \cdot \sin \alpha_{wt} \cdot \sqrt{\frac{d_{AB1}^2 - d_{b1}^2}{d_{w1}^2 - d_{b1}^2}} \quad v_{r1,AB} = 6,916 \text{ m/s}$$

$$v_{r1,B} = 2 \cdot \pi \cdot \frac{n_1}{60} \cdot \frac{d_{w1}}{2000} \cdot \sin \alpha_{wt} \cdot \sqrt{\frac{d_{B1}^2 - d_{b1}^2}{d_{w1}^2 - d_{b1}^2}} \quad v_{r1,B} = 8,998 \text{ m/s}$$

$$v_{r1,C} = 2 \cdot \pi \cdot \frac{n_1}{60} \cdot \frac{d_{w1}}{2000} \cdot \sin \alpha_{wt} \cdot \sqrt{\frac{d_{C1}^2 - d_{b1}^2}{d_{w1}^2 - d_{b1}^2}} \quad v_{r1,C} = 11,985 \text{ m/s}$$

$$v_{r1,D} = 2 \cdot \pi \cdot \frac{n_1}{60} \cdot \frac{d_{w1}}{2000} \cdot \sin \alpha_{wt} \cdot \sqrt{\frac{d_{D1}^2 - d_{b1}^2}{d_{w1}^2 - d_{b1}^2}} \quad v_{r1,D} = 14,971 \text{ m/s}$$

$$v_{r1,DE} = 2 \cdot \pi \cdot \frac{n_1}{60} \cdot \frac{d_{w1}}{2000} \cdot \sin \alpha_{wt} \cdot \sqrt{\frac{d_{DE1}^2 - d_{b1}^2}{d_{w1}^2 - d_{b1}^2}} \quad v_{r1,DE} = 17,053 \text{ m/s}$$

$$v_{r1,E} = 2 \cdot \pi \cdot \frac{n_1}{60} \cdot \frac{d_{w1}}{2000} \cdot \sin \alpha_{wt} \cdot \sqrt{\frac{d_{E1}^2 - d_{b1}^2}{d_{w1}^2 - d_{b1}^2}} \quad v_{r1,E} = 19,135 \text{ m/s}$$

$$v_{r2,A} = 2 \cdot \pi \cdot \frac{n_1}{60 \cdot u} \cdot \frac{d_{w2}}{2000} \cdot \sin \alpha_{wt} \cdot \sqrt{\frac{d_{A2}^2 - d_{b2}^2}{d_{w2}^2 - d_{b2}^2}} \quad v_{r2,A} = 19,135 \text{ m/s}$$

$$v_{r2,AB} = 2 \cdot \pi \cdot \frac{n_1}{60 \cdot u} \cdot \frac{d_{w2}}{2000} \cdot \sin \alpha_{wt} \cdot \sqrt{\frac{d_{AB2}^2 - d_{b2}^2}{d_{w2}^2 - d_{b2}^2}} \quad v_{r2,AB} = 17,053 \text{ m/s}$$

$$v_{r2,B} = 2 \cdot \pi \cdot \frac{n_1}{60 \cdot u} \cdot \frac{d_{w2}}{2000} \cdot \sin \alpha_{wt} \cdot \sqrt{\frac{d_{B2}^2 - d_{b2}^2}{d_{w2}^2 - d_{b2}^2}} \quad v_{r2,B} = 14,971 \text{ m/s}$$

$$v_{r2,C} = 2 \cdot \pi \cdot \frac{n_1}{60 \cdot u} \cdot \frac{d_{w2}}{2000} \cdot \sin \alpha_{wt} \cdot \sqrt{\frac{d_{C2}^2 - d_{b2}^2}{d_{w2}^2 - d_{b2}^2}} \quad v_{r2,C} = 11,985 \text{ m/s}$$

$$v_{r2,D} = 2 \cdot \pi \cdot \frac{n_1}{60 \cdot u} \cdot \frac{d_{w2}}{2000} \cdot \sin \alpha_{wt} \cdot \sqrt{\frac{d_{D2}^2 - d_{b2}^2}{d_{w2}^2 - d_{b2}^2}} \quad v_{r2,D} = 8,998 \text{ m/s}$$

$$v_{r2,DE} = 2 \cdot \pi \cdot \frac{n_1}{60 \cdot u} \cdot \frac{d_{w2}}{2000} \cdot \sin \alpha_{wt} \cdot \sqrt{\frac{d_{DE2}^2 - d_{b2}^2}{d_{w2}^2 - d_{b2}^2}} \quad v_{r2,DE} = 6,916 \text{ m/s}$$

$$v_{r2,E} = 2 \cdot \pi \cdot \frac{n_1}{60 \cdot u} \cdot \frac{d_{w2}}{2000} \cdot \sin \alpha_{wt} \cdot \sqrt{\frac{d_{E2}^2 - d_{b2}^2}{d_{w2}^2 - d_{b2}^2}} \quad v_{r2,E} = 4,834 \text{ m/s}$$

$$v_{g,A} = v_{r1,A} - v_{r2,A} \quad v_{g,A} = -14,300 \text{ m/s}$$

$$v_{g,AB} = v_{r1,AB} - v_{r2,AB} \quad v_{g,AB} = -10,137 \text{ m/s}$$

$$v_{g,B} = v_{r1,B} - v_{r2,B} \quad v_{g,B} = -5,974 \text{ m/s}$$

$$v_{g,C} = v_{r1,C} - v_{r2,C} \quad v_{g,C} = 0 \text{ m/s}$$

$$v_{g,D} = v_{r1,D} - v_{r2,D} \quad v_{g,D} = 5,974 \text{ m/s}$$

$$v_{g,DE} = v_{r1,DE} - v_{r2,DE} \quad v_{g,DE} = 10,137 \text{ m/s}$$

$$v_{g,E} = v_{r1,E} - v_{r2,E} \quad v_{g,E} = 14,300 \text{ m/s}$$

$$v_{\Sigma,A} = v_{r1,A} + v_{r2,A} \quad v_{\Sigma,A} = 23,969 \text{ m/s}$$

$$v_{\Sigma,AB} = v_{r1,AB} + v_{r2,AB} \quad v_{\Sigma,AB} = 23,969 \text{ m/s}$$

$$v_{\Sigma,B} = v_{r1,B} + v_{r2,B} \quad v_{\Sigma,B} = 23,969 \text{ m/s}$$

$$V_{\Sigma,C} = V_{r1,C} + V_{r2,C}$$

$$V_{\Sigma,C} = 23,969 \text{ m/s}$$

$$V_{\Sigma,D} = V_{r1,D} + V_{r2,D}$$

$$V_{\Sigma,D} = 23,969 \text{ m/s}$$

$$V_{\Sigma,DE} = V_{r1,DE} + V_{r2,DE}$$

$$V_{\Sigma,DE} = 23,969 \text{ m/s}$$

$$V_{\Sigma,E} = V_{r1,E} + V_{r2,E}$$

$$V_{\Sigma,E} = 23,969 \text{ m/s}$$

effective arithmetic mean roughness value:

$$Ra = 0,5 \cdot (Ra_1 + Ra_2)$$

$$Ra = 0,90 \text{ } \mu\text{m}$$

B.2.4 Calculation of lubricant data

$$A = \frac{\log[\log(v_{40} + 0,7) / \log(v_{100} + 0,7)]}{\log(313 / 373)}$$

$$A = -3,385$$

$$B = \log[\log(v_{40} + 0,7)] - A \cdot \log(313)$$

$$B = 8,815$$

$$\log[\log(v_{\theta\text{oil}} + 0,7)] = A \cdot \log(\theta_{\text{oil}} + 273) + B$$

$$v_{\theta\text{oil}} = 24,825 \text{ mm}^2/\text{s}$$

$$\rho_{\theta\text{oil}} = \rho_{15} \cdot \left[1 - 0,7 \cdot \frac{(\theta_{\text{oil}} + 273) - 289}{\rho_{15}} \right]$$

$$\rho_{\theta\text{oil}} = 843,2 \text{ kg/m}^3$$

$$\eta_{\theta\text{oil}} = 10^{-6} \cdot v_{\text{oil}} \cdot \rho_{\text{oil}}$$

$$\eta_{\theta\text{oil}} = 0,021 \text{ N}\cdot\text{s/m}^2$$

$X_L = 1,0$ for mineral oil (see Table 3)

$$\log[\log(v_{38} + 0,7)] = A \cdot \log(38 + 273) + B$$

$$v_{38} = 236,242 \text{ mm}^2/\text{s}$$

$$\rho_{38} = \rho_{15} \cdot \left[1 - 0,7 \cdot \frac{(38 + 273) - 289}{\rho_{15}} \right]$$

$$\rho_{38} = 879,6 \text{ kg/m}^3$$

$$\eta_{38} = 10^{-6} \cdot v_{38} \cdot \rho_{38}$$

$$\eta_{38} = 0,208 \text{ N}\cdot\text{s/m}^2$$

$$\alpha_{38} = 2,657 \cdot 10^{-8} \cdot \eta_{38}^{0,1348}$$

$$\alpha_{38} = 2,15 \cdot 10^{-8} \text{ m}^2/\text{N}$$

$X_S = 1,2$ for injection lubrication

B.2.5 Calculation of the material parameter

mean coefficient of friction:

$$X_R = 2,2 \cdot \left(\frac{Ra}{\rho_{n,C}} \right)^{0,25}$$

$$X_R = 1,025$$

$$K_{By} = 1,0 \quad \text{for } \varepsilon_y < 2$$

$$\mu_m = 0,045 \cdot \left(\frac{K_A \cdot K_v \cdot K_{Ha} \cdot K_{H\beta} \cdot F_{bt} \cdot K_{By}}{b \cdot v_{\Sigma,C} \cdot \rho_{n,C}} \right)^{0,2} \cdot (10^3 \cdot \eta_{\text{oil}})^{-0,05} \cdot X_R \cdot X_L \quad \mu_m = 0,048$$

bulk temperature:

$$H_v = (\varepsilon_1^2 + \varepsilon_2^2 + 1 - \varepsilon_\alpha) \cdot \left(\frac{1}{z_1} + \frac{1}{z_2} \right) \cdot \frac{\pi}{\cos \beta_b} \quad \text{for } \varepsilon_\alpha < 2 \quad H_v = 0,204$$

$$\varepsilon_{\max} = \varepsilon_1 = \varepsilon_2$$

$$X_{Ca} = 1,0 \quad \text{for no profile modification}$$

$$\theta_M = \theta_{\text{oil}} + 7400 \cdot \left(\frac{P \cdot \mu_m \cdot H_v}{a \cdot b} \right)^{0,72} \cdot \frac{X_S}{1,2 \cdot X_{Ca}} \quad \theta_M = 153,6 \text{ }^\circ\text{C}$$

material parameter:

$$\log[\log(v_{\theta M} + 0,7)] = A \cdot \log(\theta_M + 273) + B \quad v_{\theta M} = 5,824 \text{ mm}^2/\text{s}$$

$$\rho_{\theta M} = \rho_{15} \cdot \left[1 - 0,7 \cdot \frac{(\theta_M + 273) - 289}{\rho_{15}} \right] \quad \rho_{\theta M} = 798,7 \text{ kg/m}^3$$

$$\eta_{\theta M} = 10^{-6} \cdot v_{\theta M} \cdot \rho_{\theta M} \quad \eta_{\theta M} = 0,005 \text{ N}\cdot\text{s/m}^2$$

$$\alpha_{\theta M} = \alpha_{38} \cdot \left[1 + 516 \cdot \left(\frac{1}{\theta_M + 273} - \frac{1}{311} \right) \right] \quad \alpha_{\theta M} = 1,183 \cdot 10^{-8} \text{ m}^2/\text{N}$$

$$G_M = 10^6 \cdot \alpha_{\theta M} \cdot E_r \quad G_M = 2678,6$$

B.2.6 Calculation of the velocity parameter

$$U_A = \eta_{\theta M} \cdot \frac{v_{\Sigma,A}}{2000 \cdot E_r \cdot \rho_{n,A}} \quad U_A = 2,005 \cdot 10^{-11}$$

$$U_{AB} = \eta_{\theta M} \cdot \frac{v_{\Sigma,AB}}{2000 \cdot E_r \cdot \rho_{n,AB}} \quad U_{AB} = 1,572 \cdot 10^{-11}$$

$$U_B = \eta_{\theta M} \cdot \frac{v_{\Sigma,B}}{2000 \cdot E_r \cdot \rho_{n,B}} \quad U_B = 1,377 \cdot 10^{-11}$$

$$U_C = \eta_{\theta M} \cdot \frac{v_{\Sigma,C}}{2000 \cdot E_r \cdot \rho_{n,C}} \quad U_C = 1,291 \cdot 10^{-11}$$

$$U_D = \eta_{\theta M} \cdot \frac{V_{\Sigma,D}}{2000 \cdot E_r \cdot \rho_{n,D}} \quad U_D = 1,377 \cdot 10^{-11}$$

$$U_{DE} = \eta_{\theta M} \cdot \frac{V_{\Sigma,DE}}{2000 \cdot E_r \cdot \rho_{n,DE}} \quad U_{DE} = 1,572 \cdot 10^{-11}$$

$$U_E = \eta_{\theta M} \cdot \frac{V_{\Sigma,E}}{2000 \cdot E_r \cdot \rho_{n,E}} \quad U_E = 2,005 \cdot 10^{-11}$$

B.2.7 Calculation of the load parameter

$$W_A = \frac{\rho_{\text{dyn},A}^2 \cdot 2 \cdot \pi}{E_r^2} \quad W_A = 1,439 \cdot 10^{-4}$$

$$W_{AB} = \frac{\rho_{\text{dyn},AB}^2 \cdot 2 \cdot \pi}{E_r^2} \quad W_{AB} = 1,694 \cdot 10^{-4}$$

$$W_B = \frac{\rho_{\text{dyn},B}^2 \cdot 2 \cdot \pi}{E_r^2} \quad W_B = 2,966 \cdot 10^{-4}$$

$$W_C = \frac{\rho_{\text{dyn},C}^2 \cdot 2 \cdot \pi}{E_r^2} \quad W_C = 2,781 \cdot 10^{-4}$$

$$W_D = \frac{\rho_{\text{dyn},D}^2 \cdot 2 \cdot \pi}{E_r^2} \quad W_D = 2,966 \cdot 10^{-4}$$

$$W_{DE} = \frac{\rho_{\text{dyn},DE}^2 \cdot 2 \cdot \pi}{E_r^2} \quad W_{DE} = 1,694 \cdot 10^{-4}$$

$$W_E = \frac{\rho_{\text{dyn},E}^2 \cdot 2 \cdot \pi}{E_r^2} \quad W_E = 1,439 \cdot 10^{-4}$$

B.2.8 Calculation of the sliding parameter

local flash temperature:

$$\theta_{fl,A} = \frac{\sqrt{\pi}}{2} \cdot \frac{10^6 \cdot \mu_m \cdot \rho_{\text{dyn},A} \cdot |v_{g,A}|}{B_{M1} \sqrt{v_{r1,A}} + B_{M2} \sqrt{v_{r2,A}}} \cdot \sqrt{8 \cdot \rho_{n,A} \cdot \frac{\rho_{\text{dyn},A}}{1000 \cdot E_r}} \quad \theta_{fl,A} = 175,3 \text{ } ^\circ\text{C}$$

$$\theta_{fl,AB} = \frac{\sqrt{\pi}}{2} \cdot \frac{10^6 \cdot \mu_m \cdot \rho_{\text{dyn},AB} \cdot |v_{g,AB}|}{B_{M1} \sqrt{v_{r1,AB}} + B_{M2} \sqrt{v_{r2,AB}}} \cdot \sqrt{8 \cdot \rho_{n,AB} \cdot \frac{\rho_{\text{dyn},AB}}{1000 \cdot E_r}} \quad \theta_{fl,AB} = 154,1 \text{ } ^\circ\text{C}$$

$$\theta_{fl,B} = \frac{\sqrt{\pi}}{2} \cdot \frac{10^6 \cdot \mu_m \cdot \rho_{dyn,B} \cdot |v_{g,B}|}{B_{M1}\sqrt{v_{r1,B}} + B_{M2}\sqrt{v_{r2,B}}} \cdot \sqrt{8 \cdot \rho_{n,B} \cdot \frac{\rho_{dyn,B}}{1000 \cdot E_r}}$$

$$\theta_{fl,B} = 145,4 \text{ } ^\circ\text{C}$$

$$\theta_{fl,C} = \frac{\sqrt{\pi}}{2} \cdot \frac{10^6 \cdot \mu_m \cdot \rho_{dyn,C} \cdot |v_{g,C}|}{B_{M1}\sqrt{v_{r1,C}} + B_{M2}\sqrt{v_{r2,C}}} \cdot \sqrt{8 \cdot \rho_{n,C} \cdot \frac{\rho_{dyn,C}}{1000 \cdot E_r}}$$

$$\theta_{fl,C} = 0 \text{ } ^\circ\text{C}$$

$$\theta_{fl,D} = \frac{\sqrt{\pi}}{2} \cdot \frac{10^6 \cdot \mu_m \cdot \rho_{dyn,D} \cdot |v_{g,D}|}{B_{M1}\sqrt{v_{r1,D}} + B_{M2}\sqrt{v_{r2,D}}} \cdot \sqrt{8 \cdot \rho_{n,D} \cdot \frac{\rho_{dyn,D}}{1000 \cdot E_r}}$$

$$\theta_{fl,D} = 145,4 \text{ } ^\circ\text{C}$$

$$\theta_{fl,DE} = \frac{\sqrt{\pi}}{2} \cdot \frac{10^6 \cdot \mu_m \cdot \rho_{dyn,DE} \cdot |v_{g,DE}|}{B_{M1}\sqrt{v_{r1,DE}} + B_{M2}\sqrt{v_{r2,DE}}} \cdot \sqrt{8 \cdot \rho_{n,DE} \cdot \frac{\rho_{dyn,DE}}{1000 \cdot E_r}}$$

$$\theta_{fl,DE} = 154,1 \text{ } ^\circ\text{C}$$

$$\theta_{fl,E} = \frac{\sqrt{\pi}}{2} \cdot \frac{10^6 \cdot \mu_m \cdot \rho_{dyn,E} \cdot |v_{g,E}|}{B_{M1}\sqrt{v_{r1,E}} + B_{M2}\sqrt{v_{r2,E}}} \cdot \sqrt{8 \cdot \rho_{n,E} \cdot \frac{\rho_{dyn,E}}{1000 \cdot E_r}}$$

$$\theta_{fl,E} = 175,3 \text{ } ^\circ\text{C}$$

local contact temperature as sum of bulk and local flash temperature:

$$\theta_{B,A} = \theta_M + \theta_{fl,A} \quad \theta_{B,A} = 328,9 \text{ } ^\circ\text{C}$$

$$\theta_{B,AB} = \theta_M + \theta_{fl,AB} \quad \theta_{B,AB} = 307,7 \text{ } ^\circ\text{C}$$

$$\theta_{B,B} = \theta_M + \theta_{fl,B} \quad \theta_{B,B} = 299,0 \text{ } ^\circ\text{C}$$

$$\theta_{B,C} = \theta_M + \theta_{fl,C} \quad \theta_{B,C} = 153,6 \text{ } ^\circ\text{C}$$

$$\theta_{B,D} = \theta_M + \theta_{fl,D} \quad \theta_{B,D} = 299,0 \text{ } ^\circ\text{C}$$

$$\theta_{B,DE} = \theta_M + \theta_{fl,DE} \quad \theta_{B,DE} = 307,7 \text{ } ^\circ\text{C}$$

$$\theta_{B,E} = \theta_M + \theta_{fl,E} \quad \theta_{B,E} = 328,9 \text{ } ^\circ\text{C}$$

local sliding parameter:

$$\log[\log(v_{\theta B,A} + 0,7)] = A \cdot \log(\theta_{B,A} + 273) + B \quad v_{\theta B,A} = 1,095 \text{ mm}^2/\text{s}$$

$$\log[\log(v_{\theta B,AB} + 0,7)] = A \cdot \log(\theta_{B,AB} + 273) + B \quad v_{\theta B,AB} = 1,235 \text{ mm}^2/\text{s}$$

$$\log[\log(v_{\theta B,B} + 0,7)] = A \cdot \log(\theta_{B,B} + 273) + B \quad v_{\theta B,B} = 1,304 \text{ mm}^2/\text{s}$$

$$\log[\log(v_{\theta B,C} + 0,7)] = A \cdot \log(\theta_{B,C} + 273) + B \quad v_{\theta B,C} = 5,824 \text{ mm}^2/\text{s}$$

$$\log[\log(v_{\theta B,D} + 0,7)] = A \cdot \log(\theta_{B,D} + 273) + B \quad v_{\theta B,D} = 1,304 \text{ mm}^2/\text{s}$$

$$\log[\log(v_{\theta B,DE} + 0,7)] = A \cdot \log(\theta_{B,DE} + 273) + B \quad v_{\theta B,DE} = 1,235 \text{ mm}^2/\text{s}$$

$$\log[\log(v_{\theta B,E} + 0,7)] = A \cdot \log(\theta_{B,E} + 273) + B \quad v_{\theta B,E} = 1,095 \text{ mm}^2/\text{s}$$

$$\rho_{\theta B,A} = \rho_{15} \cdot \left[1 - 0,7 \cdot \frac{(\theta_{B,A} + 273) - 289}{\rho_{15}} \right]$$

$$\rho_{\theta B,A} = 676,0 \text{ kg/m}^3$$

$$\rho_{\theta B,AB} = \rho_{15} \cdot \left[1 - 0,7 \cdot \frac{(\theta_{B,AB} + 273) - 289}{\rho_{15}} \right]$$

$$\rho_{\theta B,AB} = 690,8 \text{ kg/m}^3$$

$$\rho_{\theta B,B} = \rho_{15} \cdot \left[1 - 0,7 \cdot \frac{(\theta_{B,B} + 273) - 289}{\rho_{15}} \right]$$

$$\rho_{\theta B,B} = 696,9 \text{ kg/m}^3$$

$$\rho_{\theta B,C} = \rho_{15} \cdot \left[1 - 0,7 \cdot \frac{(\theta_{B,C} + 273) - 289}{\rho_{15}} \right]$$

$$\rho_{\theta B,C} = 798,7 \text{ kg/m}^3$$

$$\rho_{\theta B,D} = \rho_{15} \cdot \left[1 - 0,7 \cdot \frac{(\theta_{B,D} + 273) - 289}{\rho_{15}} \right]$$

$$\rho_{\theta B,D} = 696,9 \text{ kg/m}^3$$

$$\rho_{\theta B,DE} = \rho_{15} \cdot \left[1 - 0,7 \cdot \frac{(\theta_{B,DE} + 273) - 289}{\rho_{15}} \right]$$

$$\rho_{\theta B,DE} = 690,8 \text{ kg/m}^3$$

$$\rho_{\theta B,E} = \rho_{15} \cdot \left[1 - 0,7 \cdot \frac{(\theta_{B,E} + 273) - 289}{\rho_{15}} \right]$$

$$\rho_{\theta B,E} = 676,0 \text{ kg/m}^3$$

$$\eta_{\theta B,A} = 10^{-6} \cdot \nu_{\theta B,A} \cdot \rho_{\theta B,A}$$

$$\eta_{\theta B,A} = 7,400 \cdot 10^{-4} \text{ N}\cdot\text{s/m}^2$$

$$\eta_{\theta B,AB} = 10^{-6} \cdot \nu_{\theta B,AB} \cdot \rho_{\theta B,AB}$$

$$\eta_{\theta B,AB} = 8,532 \cdot 10^{-4} \text{ N}\cdot\text{s/m}^2$$

$$\eta_{\theta B,B} = 10^{-6} \cdot \nu_{\theta B,B} \cdot \rho_{\theta B,B}$$

$$\eta_{\theta B,B} = 9,084 \cdot 10^{-4} \text{ N}\cdot\text{s/m}^2$$

$$\eta_{\theta B,C} = 10^{-6} \cdot \nu_{\theta B,C} \cdot \rho_{\theta B,C}$$

$$\eta_{\theta B,C} = 0,005 \text{ N}\cdot\text{s/m}^2$$

$$\eta_{\theta B,D} = 10^{-6} \cdot \nu_{\theta B,D} \cdot \rho_{\theta B,D}$$

$$\eta_{\theta B,D} = 9,084 \cdot 10^{-4} \text{ N}\cdot\text{s/m}^2$$

$$\eta_{\theta B,DE} = 10^{-6} \cdot \nu_{\theta B,DE} \cdot \rho_{\theta B,DE}$$

$$\eta_{\theta B,DE} = 8,532 \cdot 10^{-4} \text{ N}\cdot\text{s/m}^2$$

$$\eta_{\theta B,E} = 10^{-6} \cdot \nu_{\theta B,E} \cdot \rho_{\theta B,E}$$

$$\eta_{\theta B,E} = 7,400 \cdot 10^{-4} \text{ N}\cdot\text{s/m}^2$$

$$\alpha_{\theta B,A} = \alpha_{38} \cdot \left[1 + 516 \cdot \left(\frac{1}{\theta_{B,A} + 273} - \frac{1}{311} \right) \right]$$

$$\alpha_{\theta B,A} = 4,260 \cdot 10^{-9} \text{ m}^2/\text{N}$$

$$\alpha_{\theta B,AB} = \alpha_{38} \cdot \left[1 + 516 \cdot \left(\frac{1}{\theta_{B,AB} + 273} - \frac{1}{311} \right) \right]$$

$$\alpha_{\theta B,AB} = 4,931 \cdot 10^{-9} \text{ m}^2/\text{N}$$

$$\alpha_{\theta B,B} = \alpha_{38} \cdot \left[1 + 516 \cdot \left(\frac{1}{\theta_{B,B} + 273} - \frac{1}{311} \right) \right]$$

$$\alpha_{\theta B,B} = 5,223 \cdot 10^{-9} \text{ m}^2/\text{N}$$

$$\alpha_{\theta B,C} = \alpha_{38} \cdot \left[1 + 516 \cdot \left(\frac{1}{\theta_{B,C} + 273} - \frac{1}{311} \right) \right] \quad \alpha_{\theta B,C} = 1,183 \cdot 10^{-8} \text{ m}^2/\text{N}$$

$$\alpha_{\theta B,D} = \alpha_{38} \cdot \left[1 + 516 \cdot \left(\frac{1}{\theta_{B,D} + 273} - \frac{1}{311} \right) \right] \quad \alpha_{\theta B,D} = 5,223 \cdot 10^{-9} \text{ m}^2/\text{N}$$

$$\alpha_{\theta B,DE} = \alpha_{38} \cdot \left[1 + 516 \cdot \left(\frac{1}{\theta_{B,DE} + 273} - \frac{1}{311} \right) \right] \quad \alpha_{\theta B,DE} = 4,931 \cdot 10^{-9} \text{ m}^2/\text{N}$$

$$\alpha_{\theta B,E} = \alpha_{38} \cdot \left[1 + 516 \cdot \left(\frac{1}{\theta_{B,E} + 273} - \frac{1}{311} \right) \right] \quad \alpha_{\theta B,E} = 4,260 \cdot 10^{-9} \text{ m}^2/\text{N}$$

$$S_{GF,A} = \frac{\alpha_{\theta B,A} \cdot \eta_{\theta B,A}}{\alpha_{\theta M} \cdot \eta_{\theta M}} \quad S_{GF,A} = 0,057$$

$$S_{GF,AB} = \frac{\alpha_{\theta B,AB} \cdot \eta_{\theta B,AB}}{\alpha_{\theta M} \cdot \eta_{\theta M}} \quad S_{GF,AB} = 0,076$$

$$S_{GF,B} = \frac{\alpha_{\theta B,B} \cdot \eta_{\theta B,B}}{\alpha_{\theta M} \cdot \eta_{\theta M}} \quad S_{GF,B} = 0,086$$

$$S_{GF,C} = \frac{\alpha_{\theta B,C} \cdot \eta_{\theta B,C}}{\alpha_{\theta M} \cdot \eta_{\theta M}} \quad S_{GF,C} = 1,000$$

$$S_{GF,D} = \frac{\alpha_{\theta B,D} \cdot \eta_{\theta B,D}}{\alpha_{\theta M} \cdot \eta_{\theta M}} \quad S_{GF,D} = 0,086$$

$$S_{GF,DE} = \frac{\alpha_{\theta B,DE} \cdot \eta_{\theta B,DE}}{\alpha_{\theta M} \cdot \eta_{\theta M}} \quad S_{GF,DE} = 0,076$$

$$S_{GF,E} = \frac{\alpha_{\theta B,E} \cdot \eta_{\theta B,E}}{\alpha_{\theta M} \cdot \eta_{\theta M}} \quad S_{GF,E} = 0,057$$

B.2.9 Calculation of the lubricant film thickness

$$h_A = 1600 \cdot \rho_{n,A} \cdot G_M^{0,6} \cdot U_A^{0,7} \cdot W_A^{-0,13} \cdot S_{GF,A}^{0,22} \quad h_A = 0,122 \text{ } \mu\text{m}$$

$$h_{AB} = 1600 \cdot \rho_{n,AB} \cdot G_M^{0,6} \cdot U_{AB}^{0,7} \cdot W_{AB}^{-0,13} \cdot S_{GF,AB}^{0,22} \quad h_{AB} = 0,137 \text{ } \mu\text{m}$$

$$h_B = 1600 \cdot \rho_{n,B} \cdot G_M^{0,6} \cdot U_B^{0,7} \cdot W_B^{-0,13} \cdot S_{GF,B}^{0,22} \quad h_B = 0,136 \text{ } \mu\text{m}$$

$$h_C = 1600 \cdot \rho_{n,C} \cdot G_M^{0,6} \cdot U_C^{0,7} \cdot W_C^{-0,13} \cdot S_{GF,C}^{0,22} \quad h_C = 0,241 \text{ } \mu\text{m}$$

$$h_D = 1600 \cdot \rho_{n,D} \cdot G_M^{0,6} \cdot U_D^{0,7} \cdot W_D^{-0,13} \cdot S_{GF,D}^{0,22} \quad h_D = 0,136 \mu\text{m}$$

$$h_{DE} = 1600 \cdot \rho_{n,DE} \cdot G_M^{0,6} \cdot U_{DE}^{0,7} \cdot W_{DE}^{-0,13} \cdot S_{GF,DE}^{0,22} \quad h_{DE} = 0,137 \mu\text{m}$$

$$h_E = 1600 \cdot \rho_{n,E} \cdot G_M^{0,6} \cdot U_E^{0,7} \cdot W_E^{-0,13} \cdot S_{GF,E}^{0,22} \quad h_E = 0,122 \mu\text{m}$$

B.2.10 Calculation of the specific lubricant film thickness

$$\lambda_{GF,A} = \frac{h_A}{Ra} \quad \lambda_{GF,A} = 0,136$$

$$\lambda_{GF,AB} = \frac{h_{AB}}{Ra} \quad \lambda_{GF,AB} = 0,153$$

$$\lambda_{GF,B} = \frac{h_B}{Ra} \quad \lambda_{GF,B} = 0,152$$

$$\lambda_{GF,C} = \frac{h_C}{Ra} \quad \lambda_{GF,C} = 0,267$$

$$\lambda_{GF,D} = \frac{h_D}{Ra} \quad \lambda_{GF,D} = 0,152$$

$$\lambda_{GF,DE} = \frac{h_{DE}}{Ra} \quad \lambda_{GF,DE} = 0,153$$

$$\lambda_{GF,E} = \frac{h_E}{Ra} \quad \lambda_{GF,E} = 0,136$$

$$\lambda_{GF,\min} = \lambda_{GF,A} = \lambda_{GF,E} \quad \lambda_{GF,\min} = 0,136$$

B.3 Calculation of the permissible specific lubricant film thickness

Calculation of the permissible specific lubricant film thickness from the test result of the FZG-FVA micropitting test (Method B) with the reference test gears type C-GF:

The calculation of the reference value λ_{GFT} is done for point A, because the minimum specific lubricant film thickness for gear type C is always at point A! All data of the reference test gears type C-GF have the subscript "Ref".

NOTE The permissible specific lubricant film thickness λ_{GFP} can also be determined from Figure A.1.

B.3.1 Input data of the test gears type C-GF

number of teeth of pinion: $Z_{1Ref} = 16$

number of teeth of wheel: $Z_{2Ref} = 24$

transverse module: $m_{nRef} = m_{tRef} = 4,5 \text{ mm}$

tip diameter of pinion:	$d_{a1Ref} = 82,45 \text{ mm}$
tip diameter of wheel:	$d_{a2Ref} = 118,35 \text{ mm}$
addendum modification factor of pinion:	$x_{1Ref} = 0,1817$
addendum modification factor of wheel:	$x_{2Ref} = 0,1716$
face width:	$b_{Ref} = 14 \text{ mm}$
base helix angle:	$\beta_{bRef} = \beta_{Ref} = 0^\circ$
transverse pressure angle:	$\alpha_{tRef} = \alpha_{nRef} = 20^\circ$
centre distance:	$a_{Ref} = 91,5 \text{ mm}$
arithmetic mean roughness value of pinion:	$Ra_{1Ref} = 0,50 \mu\text{m}$
arithmetic mean roughness value of wheel:	$Ra_{2Ref} = 0,50 \mu\text{m}$
tooth flank modifications:	no modifications
modulus of elasticity of pinion:	$E_{1Ref} = 206000 \text{ N/mm}^2$
modulus of elasticity of wheel:	$E_{2Ref} = 206000 \text{ N/mm}^2$
Poisson's ratio of pinion:	$\nu_{1Ref} = 0,3$
Poisson's ratio of wheel:	$\nu_{2Ref} = 0,3$
specific heat conductivity of pinion:	$\lambda_{M1Ref} = 45 \text{ W/(mK)}$
specific heat conductivity of wheel:	$\lambda_{M2Ref} = 45 \text{ W/(mK)}$
specific heat per unit mass of pinion:	$c_{M1Ref} = 440 \text{ J/(kgK)}$
specific heat per unit mass of wheel:	$c_{M2Ref} = 440 \text{ J/(kgK)}$
density of pinion:	$\rho_{M1Ref} = 7800 \text{ kg/m}^3$
density of wheel:	$\rho_{M2Ref} = 7800 \text{ kg/m}^3$
nominal torque at the pinion for SKS 8:	$T_{1Ref} = 171,6 \text{ Nm}$
nominal Hertzian contact stress at point A according to Method A for SKS 8:	$p_{H,A,A} = 1191 \text{ N/mm}^2$
application factor:	$K_{ARef} = 1,0$
dynamic factor:	$K_{VRef} = 1,0$
transverse load factor:	$K_{H\alpha Ref} = 1,0$
face load factor:	$K_{H\beta Ref} = 1,0$
rotation speed of the pinion:	$n_{1Ref} = 2250 \text{ min}^{-1}$
lubrication:	injection lubrication

B.3.2 Calculation of gear geometry type C-GF

$$d_{1Ref} = z_{1Ref} \cdot m_{tRef}$$

$$d_{1Ref} = 72,00 \text{ mm}$$

$$d_{2Ref} = z_{2Ref} \cdot m_{tRef}$$

$$d_{2Ref} = 108,00 \text{ mm}$$

$$u_{Ref} = \frac{z_{2Ref}}{z_{1Ref}}$$

$$u_{Ref} = 1,5$$

$$d_{b1Ref} = d_{1Ref} \cdot \cos \alpha_{tRef}$$

$$d_{b1Ref} = 67,658 \text{ mm}$$

$$d_{b2Ref} = d_{2Ref} \cdot \cos \alpha_{tRef}$$

$$d_{b2Ref} = 101,487 \text{ mm}$$

$$d_{w1Ref} = \frac{2 \cdot a_{Ref}}{u_{Ref} + 1}$$

$$d_{w1Ref} = 73,20 \text{ mm}$$

$$d_{w2Ref} = 2 \cdot a_{Ref} - d_{w1Ref}$$

$$d_{w2Ref} = 109,80 \text{ mm}$$

$$\alpha_{wtRef} = \arccos \left[\frac{(z_{1Ref} + z_{2Ref}) \cdot m_{tRef} \cdot \cos \alpha_{tRef}}{2 \cdot a_{Ref}} \right]$$

$$\alpha_{wtRef} = 22,439^\circ$$

$$p_{etRef} = m_{tRef} \cdot \pi \cdot \cos \alpha_{tRef}$$

$$p_{etRef} = 13,285 \text{ mm}$$

$$\varepsilon_{1Ref} = \frac{z_{1Ref}}{2 \cdot \pi} \cdot \left[\sqrt{\left(\frac{d_{a1Ref}}{d_{b1Ref}} \right)^2} - 1 - \tan \alpha_{wtRef} \right]$$

$$\varepsilon_{1Ref} = 0,722$$

$$\varepsilon_{2Ref} = \frac{z_{2Ref}}{2 \cdot \pi} \cdot \left[\sqrt{\left(\frac{d_{a2Ref}}{d_{b2Ref}} \right)^2} - 1 - \tan \alpha_{wtRef} \right]$$

$$\varepsilon_{2Ref} = 0,714$$

$$\varepsilon_{\alpha Ref} = \frac{1}{p_{etRef}} \cdot \left(\sqrt{\frac{d_{a1Ref}^2}{4} - \frac{d_{b1Ref}^2}{4}} + \sqrt{\frac{d_{a2Ref}^2}{4} - \frac{d_{b2Ref}^2}{4}} - a_{Ref} \cdot \sin \alpha_{wtRef} \right)$$

$$\varepsilon_{\alpha Ref} = 1,436$$

$$\varepsilon_{\beta Ref} = \frac{b_{Ref} \cdot \sin \beta_{Ref}}{m_{nRef} \cdot \pi}$$

$$\varepsilon_{\beta Ref} = 0$$

$$\varepsilon_{\gamma Ref} = \varepsilon_{\alpha Ref} + \varepsilon_{\beta Ref}$$

$$\varepsilon_{\gamma Ref} = 1,436$$

$$g_{\alpha Ref} = 0,5 \cdot \left(\sqrt{d_{a1Ref}^2 - d_{b1Ref}^2} + \sqrt{d_{a2Ref}^2 - d_{b2Ref}^2} \right) - a_{Ref} \cdot \sin \alpha_{wtRef}$$

$$g_{\alpha Ref} = 19,079 \text{ mm}$$

$$g_{ARef} = 0 \text{ mm}$$

$$g_{ARef} = 0 \text{ mm}$$

$$d_{A1Ref} = 2 \cdot \sqrt{\frac{d_{b1Ref}^2}{4} + \left(\sqrt{\frac{d_{a1Ref}^2}{4} - \frac{d_{b1Ref}^2}{4}} - g_{\alpha Ref} + g_{ARef} \right)^2}$$

$$d_{A1Ref} = 68,249 \text{ mm}$$

$$d_{A2Ref} = 2 \cdot \sqrt{\frac{d_{b2Ref}^2}{4} + \left(\sqrt{\frac{d_{a2Ref}^2}{4} - \frac{d_{b2Ref}^2}{4}} - g_{ARef} \right)^2} \quad d_{A2Ref} = 118,350 \text{ mm}$$

$$\rho_{t1,ARef} = \sqrt{\frac{d_{A1Ref}^2 - d_{b1Ref}^2}{4}} \quad \rho_{t1,ARef} = 4,482 \text{ mm}$$

$$\rho_{t1,CRef} = \sqrt{\frac{d_{w1Ref}^2 - d_{b1Ref}^2}{4}} \quad \rho_{t1,CRef} = 13,970 \text{ mm}$$

$$\rho_{t2,ARef} = \sqrt{\frac{d_{A2Ref}^2 - d_{b2Ref}^2}{4}} \quad \rho_{t2,ARef} = 30,443 \text{ mm}$$

$$\rho_{t2,CRef} = \sqrt{\frac{d_{w2Ref}^2 - d_{b2Ref}^2}{4}} \quad \rho_{t2,CRef} = 20,955 \text{ mm}$$

$$\rho_{t,ARef} = \frac{\rho_{t1,ARef} \cdot \rho_{t2,ARef}}{\rho_{t1,ARef} + \rho_{t2,ARef}} \quad \rho_{t,ARef} = \rho_{n,ARef} = 3,907 \text{ mm}$$

$$\rho_{t,CRef} = \frac{\rho_{t1,CRef} \cdot \rho_{t2,CRef}}{\rho_{t1,CRef} + \rho_{t2,CRef}} \quad \rho_{t,CRef} = \rho_{n,CRef} = 8,382 \text{ mm}$$

B.3.3 Calculation of material data type C-GF

$$E_{rRef} = 2 \cdot \left(\frac{1 - \nu_{1Ref}^2}{E_{1Ref}} + \frac{1 - \nu_{2Ref}^2}{E_{2Ref}} \right)^{-1} \quad E_{rRef} = 226374 \text{ N/mm}^2$$

$$B_{M1Ref} = \sqrt{\lambda_{M1Ref} \cdot \rho_{M1Ref} \cdot C_{M1Ref}} \quad B_{M1Ref} = 12427,4 \text{ N/(ms}^{0,5}\text{K)}$$

$$B_{M2Ref} = \sqrt{\lambda_{M2Ref} \cdot \rho_{M2Ref} \cdot C_{M2Ref}} \quad B_{M2Ref} = 12427,4 \text{ N/(ms}^{0,5}\text{K)}$$

B.3.4 Calculation of operating conditions of FVA-FZG micropitting test

$$P_{Ref} = 2 \cdot \pi \cdot \frac{n_{1Ref}}{60} \cdot \frac{T_{1Ref}}{1000} \quad P_{Ref} = 40,43 \text{ kW}$$

$$F_{btRef} = 2000 \cdot \frac{T_{1Ref}}{d_{b1Ref}} \quad F_{btRef} = 5072,6 \text{ N}$$

$$p_{dyn,A,ARef} = p_{H,A,ARef} \cdot \sqrt{K_{ARef} \cdot K_{vRef}} \quad p_{dyn,A,ARef} = 1191 \text{ N/mm}^2$$

$$V_{r1,ARef} = 2 \cdot \pi \cdot \frac{n_{1Ref}}{60} \cdot \frac{d_{w1Ref}}{2000} \cdot \sin \alpha_{wtRef} \cdot \sqrt{\frac{d_{A1Ref}^2 - d_{b1Ref}^2}{d_{w1Ref}^2 - d_{b1Ref}^2}} \quad V_{r1,ARef} = 1,056 \text{ m/s}$$

$$V_{r1,CRef} = 2 \cdot \pi \cdot \frac{n_{1Ref}}{60} \cdot \frac{d_{w1Ref}}{2000} \cdot \sin \alpha_{wtRef} \quad V_{r1,CRef} = 3,292 \text{ m/s}$$

$$V_{r2,ARef} = 2 \cdot \pi \cdot \frac{n_{1Ref}}{60 \cdot u_{Ref}} \cdot \frac{d_{w2Ref}}{2000} \cdot \sin \alpha_{wtRef} \cdot \sqrt{\frac{d_{A2Ref}^2 - d_{b2Ref}^2}{d_{w2Ref}^2 - d_{b2Ref}^2}} \quad V_{r2,ARef} = 4,782 \text{ m/s}$$

$$V_{r2,CRef} = 2 \cdot \pi \cdot \frac{n_{1Ref}}{60 \cdot u_{Ref}} \cdot \frac{d_{w2Ref}}{2000} \cdot \sin \alpha_{wtRef} \quad V_{r2,CRef} = 3,292 \text{ m/s}$$

$$V_{g,ARef} = V_{r1,ARef} - V_{r2,ARef} \quad V_{g,ARef} = -3,726 \text{ m/s}$$

$$V_{\Sigma,ARef} = V_{r1,ARef} + V_{r2,ARef} \quad V_{\Sigma,ARef} = 5,838 \text{ m/s}$$

$$V_{\Sigma,CRef} = V_{r1,CRef} + V_{r2,CRef} \quad V_{\Sigma,CRef} = 6,583 \text{ m/s}$$

$$Ra_{Ref} = 0,5 \cdot (Ra_{1Ref} + Ra_{2Ref}) \quad Ra_{Ref} = 0,50 \text{ } \mu\text{m}$$

B.3.5 Calculation of lubricant data

$$\theta_{oilRef} = \theta_{oil} = 90 \text{ } ^\circ\text{C}$$

$$\eta_{\theta_{oilRef}} = \eta_{\theta_{oil}} = 0,021 \text{ N}\cdot\text{s/m}^2$$

$$X_{SRef} = 1,2 \quad \text{for injection lubrication}$$

B.3.6 Calculation of the permissible specific lubricant film thickness

$$X_{RRef} = 2,2 \cdot \left(\frac{Ra_{Ref}}{\rho_{n,CRef}} \right)^{0,25} \quad X_{RRef} = 1,087$$

$$K_{ByRef} = 1,0 \quad \text{for } \varepsilon_\gamma < 2$$

$$\Sigma K_{Ref} = K_{ARef} \cdot K_{VRef} \cdot K_{H\alpha Ref} \cdot K_{H\beta Ref} \cdot K_{ByRef} \quad \Sigma K_{Ref} = 1,0$$

$$\mu_{mRef} = 0,045 \cdot \left(\frac{\Sigma K_{Ref} \cdot F_{btRef}}{b_{Ref} \cdot V_{\Sigma,CRef} \cdot \rho_{n,CRef}} \right)^{0,2} \cdot (10^3 \cdot \eta_{\theta_{oilRef}})^{-0,05} \cdot X_{RRef} \cdot X_L \quad \mu_{mRef} = 0,061$$

$$H_{vRef} = (\varepsilon_{1Ref}^2 + \varepsilon_{2Ref}^2 + 1 - \varepsilon_{\alpha Ref}) \cdot \left(\frac{1}{z_{1Ref}} + \frac{1}{z_{2Ref}} \right) \cdot \frac{\pi}{\cos \beta_{bRef}} \quad \text{for } \varepsilon_\alpha < 2 \quad H_{vRef} = 0,195$$

$$X_{CaRef} = 1,0 \quad \text{for no profile modification}$$

$$\theta_{MRef} = \theta_{oilRef} + 7400 \cdot \left(\frac{P_{Ref} \cdot \mu_{mRef} \cdot H_{vRef}}{a_{Ref} \cdot b_{Ref}} \right)^{0,72} \cdot \frac{X_{SRef}}{1,2 \cdot X_{CaRef}}$$

$$\theta_{MRef} = 115,3 \text{ } ^\circ\text{C}$$

$$\log[\log(v_{\theta MRef} + 0,7)] = A \cdot \log(\theta_{MRef} + 273) + B$$

$$v_{\theta MRef} = 12,473 \text{ mm}^2/\text{s}$$

$$\rho_{\theta MRef} = \rho_{15} \cdot \left[1 - 0,7 \cdot \frac{(\theta_{MRef} + 273) - 289}{\rho_{15}} \right]$$

$$\rho_{\theta MRef} = 825,5 \text{ kg/m}^3$$

$$\eta_{\theta MRef} = 10^{-6} \cdot v_{\theta MRef} \cdot \rho_{\theta MRef}$$

$$\eta_{\theta MRef} = 0,010 \text{ N}\cdot\text{s/m}^2$$

$$\alpha_{\theta MRef} = \alpha_{38} \cdot \left[1 + 516 \cdot \left(\frac{1}{\theta_{MRef} + 273} - \frac{1}{311} \right) \right]$$

$$\alpha_{\theta MRef} = 1,440 \cdot 10^{-8} \text{ m}^2/\text{N}$$

$$G_{MRef} = 10^6 \cdot \alpha_{\theta MRef} \cdot E_{rRef}$$

$$G_{MRef} = 3258,7$$

$$U_{ARef} = \eta_{\theta MRef} \cdot \frac{v_{\Sigma, ARef}}{2000 \cdot E_{rRef} \cdot \rho_{n, ARef}}$$

$$U_{ARef} = 3,398 \cdot 10^{-11}$$

$$W_{ARef} = \frac{\rho_{dyn, ARef}^2 \cdot 2 \cdot \pi}{E_{rRef}^2}$$

$$W_{ARef} = 1,738 \cdot 10^{-4}$$

$$\theta_{fl, ARef} = \frac{\sqrt{\pi}}{2} \cdot \frac{10^6 \cdot \mu_{mRef} \cdot \rho_{dyn, ARef} \cdot |v_{g, ARef}|}{B_{M1Ref} \sqrt{v_{r1, ARef}} + B_{M2Ref} \sqrt{v_{r2, ARef}}} \cdot \sqrt{8 \cdot \rho_{n, ARef} \cdot \frac{\rho_{dyn, ARef}}{1000 \cdot E_{rRef}}}$$

$$\theta_{fl, ARef} = 77,3 \text{ } ^\circ\text{C}$$

$$\theta_{B, ARef} = \theta_{MRef} + \theta_{fl, ARef}$$

$$\theta_{B, ARef} = 192,6 \text{ } ^\circ\text{C}$$

$$\log[\log(v_{\theta B, ARef} + 0,7)] = A \cdot \log(\theta_{B, ARef} + 273) + B$$

$$v_{\theta B, ARef} = 3,335 \text{ mm}^2/\text{s}$$

$$\rho_{\theta B, ARef} = \rho_{15} \cdot \left[1 - 0,7 \cdot \frac{(\theta_{B, ARef} + 273) - 289}{\rho_{15}} \right]$$

$$\rho_{\theta B, ARef} = 771,4 \text{ kg/m}^3$$

$$\eta_{\theta B, ARef} = 10^{-6} \cdot v_{\theta B, ARef} \cdot \rho_{\theta B, ARef}$$

$$\eta_{\theta B, ARef} = 0,003 \text{ N}\cdot\text{s/m}^2$$

$$\alpha_{\theta B, ARef} = \alpha_{38} \cdot \left[1 + 516 \cdot \left(\frac{1}{\theta_{B, ARef} + 273} - \frac{1}{311} \right) \right]$$

$$\alpha_{\theta B, ARef} = 9,655 \cdot 10^{-9} \text{ m}^2/\text{N}$$

$$S_{GF, ARef} = \frac{\alpha_{\theta B, ARef} \cdot \eta_{\theta B, ARef}}{\alpha_{\theta MRef} \cdot \eta_{\theta MRef}}$$

$$S_{GF, ARef} = 0,168$$

$$h_{ARef} = 1600 \cdot \rho_{n, ARef} \cdot G_{MRef}^{0,6} \cdot U_{ARef}^{0,7} \cdot W_{ARef}^{-0,13} \cdot S_{GF, ARef}^{0,22}$$

$$h_{ARef} = 0,078 \text{ } \mu\text{m}$$

$$\lambda_{GFT} = \lambda_{GF, ARef} = \frac{h_{ARef}}{Ra_{Ref}}$$

$$\lambda_{GFT} = 0,157$$

$$\lambda_{GFP} = 1,4 \cdot W_W \cdot \lambda_{GFT}$$

$$\lambda_{GFP} = 0,219$$

B.4 Calculation of the micropitting safety factor

$$S_{\lambda} = \frac{\lambda_{GF, \min}}{\lambda_{GFP}}$$

$$S_{\lambda} = 0,62$$

Bibliography

- [1] AGMA 925-A03, Effect of Lubrication on Gear Surface Distress, 2003.
- [2] BGA-DU P602, Gear Micropitting Procedure. Test Procedure for the Evaluation of Micropitting Performance of Spur and Helical Gears. 2008.
- [3] Buzdygon, K.J., Cardis, A.B., A Short Procedure to Evaluate Micropitting Using the New AGMA Designed Gears. AGMA Fall Technical Meeting, 2004.
- [4] Det Norske Veritas, Classif. Note 41.2, Calculation of gear rating for marine transmissions. 1993.
- [5] Dowson, D.; Higginson, G.R., Elastohydrodynamic Lubrication. Pergamon Press, Oxford, 1966.
- [6] Elstopff, M.-G., Einflüsse auf die Grübchentragfähigkeit einsatzgehärteter Zahnräder bis in das höchste Zeitfestigkeitsgebiet. Dissertation Technische Universität München, 1993.
- [7] FVA-Information Sheet 54/7, Test procedure for the investigation of the micropitting capacity of gear lubricants. 1993.
- [8] ISO 10825:1995, *Gears — Wear and damage to gear teeth — Terminology*.
- [9] McGrew, J.M., et al., Elastohydrodynamic Lubrication-Preliminary Design Manual. Tech. Rep. AFAOL Tr-70-27, WP AFB, Ohio (USA), November 1970.
- [10] Oster, P., Beanspruchung der Zahnflanken unter Bedingungen der Elastohydrodynamik. Dissertation Technische Universität München, 1982.
- [11] Schrade, U., Einfluss von Verzahnungsgeometrie und Betriebsbedingungen auf die Graufleckentragfähigkeit von Zahnradgetrieben. Dissertation Technische Universität München, 2000.
- [12] Theißen, J., Eignungsnachweise von Schmierölen für Industriegetriebe. 11th International Colloquium, 13. - 15.1.1998, Technische Akademie Esslingen, 1998.
- [13] Theyse, F.H., *Die Blitztemperaturmethode nach Blok und ihre praktische Anwendung bei Zahnrädern*. Schmiertechnik 1, S. pp. 22-29, 1967.

ICS 21.200

Price based on 55 pages